Physiological Properties of Rod Photoreceptor Cells in Green-sensitive Cone Pigment Knock-in Mice

Keisuke Sakurai,[1] Akishi Onishi,[1] Hiroo Imai,[1] Osamu Chisaka,[2] Yoshiki Ueda,[3] Jiro Usukura,[4] Kei Nakatani,[5] and Yoshinori Shichida[1]

[1]Department of Biophysics, Graduate School of Science, Kyoto University and Core Research for Evolutional Science and Technology (CREST), Japan Science and Technology Agency, Kyoto 606-8502, Japan
[2]Department of Cell and Developmental Biology, Graduate School of Biostudies, Kyoto University, Kyoto 606-8501, Japan
[3]Department of Ophthalmology, School of Medicine, Kyoto University, Kyoto 606-8501, Japan
[4]Department of Anatomy and Cell Biology, School of Medicine, Nagoya University, Nagoya 466-8550, Japan
[5]Graduate School of Life and Environmental Science, University of Tsukuba and Core Research for Evolutional Science and Technology (CREST), Japan Science and Technology Agency, Tsukuba, Ibaraki 305-8572, Japan

Rod and cone photoreceptor cells that are responsible for scotopic and photopic vision, respectively, exhibit photoresponses different from each other and contain similar phototransduction proteins with distinctive molecular properties. To investigate the contribution of the different molecular properties of visual pigments to the responses of the photoreceptor cells, we have generated knock-in mice in which rod visual pigment (rhodopsin) was replaced with mouse green-sensitive cone visual pigment (mouse green). The mouse green was successfully transported to the rod outer segments, though the expression of mouse green in homozygous retina was ∼11% of rhodopsin in wild-type retina. Single-cell recordings of wild-type and homozygous rods suggested that the flash sensitivity and the single-photon responses from mouse green were three to fourfold lower than those from rhodopsin after correction for the differences in cell volume and levels of several signal transduction proteins. Subsequent measurements using heterozygous rods expressing both mouse green and rhodopsin E122Q mutant, where these pigments in the same rod cells can be selectively irradiated due to their distinctive absorption maxima, clearly showed that the photoresponse of mouse green was threefold lower than that of rhodopsin. Noise analysis indicated that the rate of thermal activations of mouse green was $1.7 \times 10^{-7}\,\mathrm{s}^{-1}$, about 860-fold higher than that of rhodopsin. The increase in thermal activation of mouse green relative to that of rhodopsin results in only 4% reduction of rod photosensitivity for bright lights, but would instead be expected to severely affect the visual threshold under dim-light conditions. Therefore, the abilities of rhodopsin to generate a large single photon response and to retain high thermal stability in darkness are factors that have been necessary for the evolution of scotopic vision.

INTRODUCTION

In the eyes of most vertebrates, there are two types of photoreceptor cells, rods and cones, which mediate scotopic (starlight to twilight) and photopic (daylight) vision, respectively. Rods are more sensitive to light than cones, while cones have faster photoresponses and adapt quicker than rods. Rods and cones have similar phototransduction proteins, though with different molecular properties, suggesting that the different photoresponses between rods and cones originates from the different properties of these phototransduction proteins (Yau, 1994; Ebrey and Koutalos, 2001; Arshavsky et al., 2002). Previously, amino acid sequences of rod and cone visual pigments have been determined, and

phylogenetic analyses concluded that an ancestral visual pigment evolved first into four groups of cone visual pigments and then the group of rod visual pigments, rhodopsin, diverged from one of the cone visual pigment groups (Okano et al., 1992). Although there are a few exceptions, rhodopsin and cone visual pigments are expressed in rods and cones, respectively. These facts suggest that rhodopsin would have acquired unique molecular properties in the course of molecular evolution so as to meet the requirement of scotopic vision where simultaneous photon absorptions by rods occur at a very low rate (Hecht et al., 1942; Barlow, 1956).

Rods are able to respond to single-photon stimuli (Baylor et al., 1979). The amplitude of the single photon response of a photoreceptor cell is dependent on how efficiently the phototransduction cascade is activated by the visual pigment. Comparison of mouse rod

Abbreviations used in this paper: ES, embryonic stem; GRK, G protein–coupled receptor kinase; GTPγS, guanosine 5′-O-(3-thiotriphosphate); ROS, rod outer segment.

and cone photoresponses by means of single cell recording has demonstrated that the amplification efficiency of the transduction cascade per activated visual pigment is at least fivefold higher in rods than in cones (Nikonov et al., 2006). Therefore, it is of interest to elucidate the contributions of rhodopsin and cone pigments to the differences in amplification efficiencies of rods and cones.

Electrophysiological studies have also demonstrated that rods exhibit a very low level of noise in the dark (Baylor et al., 1980, 1984). This property should be due in part to the extremely inert character of rhodopsin in the dark state; that is, thermal activation of a single rhodopsin molecule in amphibian rod occurs spontaneously only about once every 3,000 years at room temperature. In contrast, the dark noise of cones, especially that of red-sensitive salamander cones, is considerably higher than that of rods, and originates predominantly from spontaneous thermal activations of red-sensitive cone visual pigments (Rieke and Baylor, 2000; Sampath and Baylor, 2002). A recent study of *Xenopus* rods expressing red-sensitive cone pigments has demonstrated that the low thermal stability of red-sensitive cone visual pigments activated phototransduction in the dark, thereby resulting in reduced sensitivity and accelerated response kinetics through "light adaptation" (Kefalov et al., 2003). These results suggest that the thermal stability of visual pigment in the dark is a significant factor in determining the characteristics of rods and cones. However, for blue-sensitive and green-sensitive cones, the contribution of thermal stability of visual pigment is not prominent, because the variance in the dark current arose mostly from a higher frequency biological noise component (continuous noise) that could be attributed to a molecular source downstream of the pigment (Lamb and Simon, 1977; Rieke and Baylor, 2000; Holcman and Korenbrot, 2005). Moreover, cone visual pigments in amphibian retinas widely studied by electrophysiology contain mostly an A2 retinal as their chromophore and A2-based pigments are expected to be less stable than the A1-based visual pigments, which are used in mammalian retinas (Donner et al., 1990). Therefore, it is desirable to examine whether the thermal stability of cone visual pigments really affects the response properties of mammalian photoreceptor cells.

In the present study, we generated knock-in mice in which the endogenous rhodopsin was replaced with mouse green-sensitive cone visual pigment (mouse green) in order to investigate the contribution of visual pigments to photoresponse properties. Mouse green exhibits an absorption maximum at 510 nm, which belongs to the long wavelength–sensitive group (L group) of visual pigments that includes the human red and salamander red (Okano et al., 1992; Ebrey and Koutalos, 2001). We compared the dim-light responses and the dark noise of the knock-in rods with those of wild-type rods using suction pipette recording. In addition, to directly evaluate the contribution of visual pigment properties, we attempted to compare single photon responses generated by mouse green and rhodopsin in the same photoreceptor cells. For this purpose, we prepared heterozygous mice that have rod photoreceptor cells containing mouse green and E122Q rhodopsin, the latter of which exhibits an absorption maximum that was blue shifted by 23 nm from that of mouse green, but which generated a photoresponse similar to that of wild-type rhodopsin (Imai et al., 2007). The results showed that the amplitude of the single photon response elicited by mouse green was about one third of that elicited by wild-type rhodopsin. We also found that mouse green exhibited a rate of thermal activations in darkness that was 1.7×10^{-7} s^{-1}, $\sim$860-fold larger than for mouse rhodopsin. These results are discussed in relation to the different photoresponse properties between rods and cones.

MATERIALS AND METHODS

Generation of the Knock-in Mouse
The mouse genomic library was screened with mouse rhodopsin cDNA (GenBank/EMBL/DDBJ M55171). One of the derived genomic clones was subcloned into pBluscript KS+ as a targeting vector. The targeting vector that contained 13.1 kb of the mouse rhodopsin locus was cloned from a 129SVj genomic library. The vector construct of mouse green consisted of two arms of homologous genomic segments of mouse rhodopsin; 3.8-kb 5′-AatII/XhoI and 9.7-kb 3′-XhoI/ClaI fragments separated by the mouse green opsin cDNA sequence and 2.0-kb 3′ untranslated region (3′UTR) of rhodopsin gene containing five polyadenylation (poly(A)) signals and a *lox*P-phosphoglycerate kinase promoter-neomycin phototransperase II (neo)-*lox*P cassette. The intron inserted to the XhoI site on the 5′UTR of the mouse rhodopsin gene is a 133-bp artificial hybrid intron (Choi et al., 1991) derived from pCIneo (Promega) that was present on a 95-bp blunt fragment. The targeting vector was transferred into CMTI-1 embryonic stem (ES) cells (Cell and Molecular Technologies) by electroporation and individual neomycin-resistant clones were isolated and expanded in 48-well plates. Properly targeted ES cells were selected by Southern blot hybridized with a 5′ flanking probe and injected into 3.5-d C57BL/6J blastocysts. Chimeric mice were then bred to obtain mice in which one or both alleles of rhodopsin locus were altered. For some experiments, mouse green knock-in mice (mG/mG) were crossed with E122Q knock-in (Rh^{EQ}/Rh^{EQ}) mice in which the rhodopsin gene contained the E122Q rhodopsin mutation (Imai et al., 2007). All the experimental procedures were performed in accordance with the guidelines set by Kyoto University, and were approved by the local committee for the handling of experimental animals in the Graduate School of Science, Kyoto University.

Genotyping of knock-in lines was performed by Southern blot analysis. In brief, genomic DNA was prepared from mouse tails, and 1 μg of DNA was digested overnight with BamHI, electrophoretically fractionated in a 0.75% agarose gel, denatured, and transferred to a nylon membrane (Roche). Hybridization was done overnight using the standard protocol for the DIG-labeled DNAs. The chemiluminesence signal derived from CDP-Star (Roche) was detected by X-ray film.

The transcript was analyzed by RT-PCR from a retinal extract of 4-wk-old mice prepared using RNeasy Mini kit (QIAGEN). After

digestion of genomic DNA by DNaseI, the first strand cDNA was synthesized with a reverse primer, RhC11 (5′-TGTCATGTTCCTG-ATA-3′), complementary to the sequence immediately preceding the first poly(A) addition signal of mouse rhodopsin. The cDNA products from endogenous rhodopsin and recombinant mouse green genes were amplified by using the rhodopsin 5′ UTR (5′-AGCAGCCTTGGTCTCTGTCT-3′) and 3′ UTR (5′-GTGGATGG-ATGTCCTTTGTC-3′) primer pairs (Kodama et al., 2005).

Estimation of Protein Expression Level

Protein expression levels were estimated by spectroscopy and Western blotting. Retinas were isolated from mouse eyes, homogenized, and extracted with buffer E (1% n-dodecyl-β-D-maltoside, 140 mM NaCl, 50 mM HEPES, pH 6.5) for spectroscopy or with SDS-PAGE sample buffer (8% SDS, 0.125 M Tris/Cl [pH 6.8], 20% glycerol, 5% mercaptoethanol) for Western blotting. The concentration of visual pigment in the extract solubilized with buffer E was estimated from the maximal absorbance of a difference spectrum before and after irradiation with >500-nm light in the presence of hydroxylamine and using molar extinction coefficients of both rhodopsin and mouse green at their absorption maxima (502 and 510 nm, respectively) of 40,200 M^{-1} cm^{-1} (Imai et al., 2007) and 45,500 M^{-1} cm^{-1} (Onishi et al., 2005), respectively. The concentration of hydroxylamine in the rhodopsin extract from wild-type retinas was 100 mM, while that in the mouse green from mG/mG retinas was 10 mM. This is because mouse green is more sensitive to hydroxylamine than rhodopsin (Okano et al., 1989; Johnson et al., 1993) and it was stable only in the presence of <10 mM hydroxylamine.

The ratio of the two kinds of pigments in the heterozygous retinas can be estimated by monitoring the bleaching processes of these pigments in the presence of 200 mM hydroxylamine in the dark. Hydroxylamine bleaches these pigments by reacting with their retinylidene Schiff base chromophores, but the reaction rate is considerably faster in mouse green than in rhodopsin (Okano et al., 1989; Johnson et al., 1993). The retinal extracts were incubated in the presence of 200 mM hydroxylamine for 12 h at 20°C and then it was irradiated with >500-nm light for 5 min to completely bleach the remaining pigments in the extract. The bleaching processes for wild-type or homozygous retinas were monitored at the λ_{max} of the relevant visual pigments and were fit by a single-exponential function to estimate the time constants of hydroxylamine reaction. For the Rh/mG mice, retinal extracts from five mice were incubated with hydroxlamine and the bleaching process was monitored at 500 nm. The bleaching kinetics was fit with a double-exponential function using the estimated reaction time constants of rhodopsin and mouse green determined above. The ratio of rhodopsin and mouse green was estimated from the fitting results corrected for the different molecular extinction coefficients at 500 nm (40,200 M^{-1} cm^{-1} for rhodopsin; 43,900 M^{-1} cm^{-1} for mouse green). For the Rh^{EQ}/mG mice, retinal extracts from five mice were incubated with hydroxylamine, and the bleaching process was monitored at 498 nm, which was the isosbestic point of the spectra of E122Q rhodopsin and mouse green. The bleaching kinetics was fit with a double-exponential function using the estimated reaction time constants of E122Q rhodopsin and mouse green.

The amount of other signal transduction proteins was determined by Western blotting. Retinas were removed from the eyes, placed in 250-μl SDS-PAGE sample buffer, and homogenized by sonication for ∼10 s with a sonicator (UR-20P; TOMY SEIKO). The homogenate was subjected to electrophoresis on 12.5% polyacrylamide gels and transferred onto polyviniliden difluoride membrane for 1–1.5 h. As a standard, four diluted samples prepared from a wild-type retina homogenate were run in neighboring lanes on the same gel. After blocking with 5% (weight/volume) ECL blocking agent (GE Healthcare) in PBS (140 mM NaCl,

2.6 mM KCl, 1.8 mM KH_2PO_4, 8.1 mM Na_2HPO_4) containing 0.05% Tween 20, the proteins in the membrane were probed with primary antibodies. The antibodies were raised against the rod transducin α-subunit (Suzuki et al., 1993), PDEα- (0.2 μg/ml; Affinity BioReagents) and PDEβ- (0.2 μg/ml; Affinity BioReagents) subunits, GRK1 (1 μg/ml; Santa Cruz Biotechnology), CNG1 (1:15 dilution; PMc101; Korschen et al., 1995), rhodopsin 1D4 (1:10,000 dilution), and mouse green opsin (1:10,000 dilution, Medical and Biological Laboratories, custom antibody against N-terminal peptide of mouse green AQRLTGEQTLDHYEDS sequence; Applebury et al., 2000). Horseradish peroxidase–conjugated secondary antibodies were used at a dilution of 1:20,000, and protein bands were visualized by ECL (GE Healthcare). Integrated densities of scanned individual bands were measured with Scion Image software (Scion) and the densities of mutant samples were compared with standard intensities of the wild-type samples to estimate the relative amounts of the proteins.

Photosensitivities of Visual Pigments

Mouse rhodopsin, E122Q rhodopsin mutant (E122Q rhodopsin), and mouse green were extracted with buffer E from mouse retinas of dark-adapted wild-type, Rh^{EQ}/Rh^{EQ}, and mG/mG mice, respectively. The pigments were irradiated with 500-nm light in the presence of 100 mM hydroxylamine for rhodopsin and E122Q rhodopsin, and in the presence of 5 mM hydroxylamine for mouse green at 2°C. The light intensity was monitored with a photodiode (S1226-5BQ; Hamamatsu Photonics). The amount of pigment in the extracts was estimated from the difference spectra calculated by subtracting spectra obtained after complete bleaching by irradiation with >500-nm light from those obtained before irradiation.

Histology

Eyes were removed and fixed for 4 h in 4% paraformaldehyde in PBS at 4°C. After cryoprotection in cold 30% sucrose, the tissue was mounted with OCT compound (Tissue-Tek) and sectioned at 10-μm thickness along the vertical meridian passing through the optic nerve. Immunostaining was performed using methods described previously (Onishi et al., 2005).

For electron microscopy, whole eyeballs were hemisected and their posterior parts including the retinas were prefixed with 2% glutaraldehyde and 2% paraformaldehyde in the buffer consisting of 30 mM HEPES, 100 mM NaCl, and 2 mM $CaCl_2$ (pH 7.4) for 2 h at room temperature. They were then post-fixed with 1% O_sO_4 in the same buffer for 1 h in a conventional way (Usukura and Yamada, 1987). Fixed samples were dehydrated gradually in ascending concentrations of ethanol and embedded in epoxy resin (PolyBed 812; Polyscience Inc). Ultrathin sections were cut out and stained with uranyl acetate and lead citrate before observation.

GTPγS Binding Assays

Light-induced activation of bovine rod transducin by mouse rhodopsin and mouse green was measured by a GTPγS binding assay as described previously (Terakita et al., 1998; Onishi et al., 2005). Rod outer segment (ROS) membranes containing rhodopsin or mouse green were prepared from retinas of dark-adapted wild-type or mG/mG mice by means of the sucrose floatation method (Shichida et al., 1987). The amount of visual pigments in ROS membranes was estimated by absorption spectroscopy after extraction of pigments with buffer E. Purification of transducin from bovine ROS was performed according to the methods described previously (Tachibanaki et al., 1997). The reaction was performed in 100 μl of Ringer solution (113 mM NaCl, 3.6 mM KCl, 2.4 mM $MgCl_2$, 1.2 mM $CaCl_2$, 10 mM HEPES, 0.02 mM EDTA, pH 7.5), containing 30 nM (at 4°C) or 10 nM (at 37°C) pigment, 300 nM (at 4°C) or 100 nM (at 37°C) bovine rod transducin, 1 μM [^{35}S]GTPγS, and 1 μM GDP. The mixture was irradiated with a white light flash (SB80-DX; Nikon) that bleached

~80% of visual pigments. After the mixture was incubated for a selected time in the dark, an aliquot (20 µl) was mixed with 250 µl of stop solution (20 mM Tris/Cl, 100 mM NaCl, 25 mM MgCl$_2$, 1 µM GTPγS, pH 7.4), and then immediately filtered through a nitrocellulose membrane to trap [^{35}S]GTPγS-bound transducin. The amount of light-dependent GTPγS bound was estimated by subtracting the amount in the absence of the light stimulus from that in the presence of the light stimulus. The membrane was washed three times with 250 µl of wash solution (20 mM Tris/Cl, pH 7.4, 100 mM NaCl, 25 mM MgCl$_2$) to remove free [^{35}S]GTPγS, and was air dried. The membrane was then put into 2 ml of aqueous counting scintillant (ACSII; GE Healthcare), and the amount of bound [^{35}S]GTPγS was measured using a liquid scintillation counter (LS600IC; Beckman Coulter).

Single-Cell Recordings

Mice kept in darkness for at least 12 h were killed by cervical dislocation and the eyes were removed and washed under dim red light conditions. All subsequent steps were performed under infrared light conditions using infrared image converters. The retina was isolated, cut into small pieces, and then finely chopped. Isolated pieces of retina were stored in Locke solution at 4°C before use. A suspension of cells was transferred to a recording chamber mounted on the microscope stage (TE300; Nikon). The solution in the recording chamber was perfused and heated to a temperature of 34–37°C, which was continuously monitored with a miniature thermocouple. The perfusion Locke solution, containing 112 mM NaCl, 3.6 mM KCl, 2.4 mM MgCl$_2$, 1.2 mM CaCl$_2$, 10 mM HEPES, 20 mM NaHCO$_3$, 3 mM Na$_2$-succinate, 0.5 mM Na-glutamate, 0.02 mM EDTA, and 10 mM glucose at pH 7.4, was equilibrated with 95% O$_2$/5% CO$_2$. Individual cells were visualized under infrared light, using a CCD camera (ORCA-ER; Hamamatsu Photonics). Capillary glass was pulled and heat polished to fit the ROS diameter (~1 µm), and filled with a solution, containing 140 mM NaCl, 3.6 mM KCl, 2.4 mM MgCl$_2$, 1.2 mM CaCl$_2$, 3 mM HEPES, and 0.02 mM EDTA at pH 7.4. The bath solution was clamped by a bath clamp circuit (Baylor et al., 1984). A rod photoreceptor cell was drawn into the electrode to record the inward current of the outer segment. The circulating current was amplified by a current-to-voltage converter (Axopatch 200B; Axon Instruments), low-pass filtered by the Axopatch four-pole Bessel filter with a cutoff frequency of 1 kHz and by an eight-pole Bessel filter with a cutoff frequency of 30 Hz (900L8L; Frequency Devices), digitized at 400 Hz, and recorded with a pClamp 8.2 acquisition system (Axon Instruments) running on a personal computer. Unpolarized 20-ms light flashes were delivered from a 500-W xenon lamp (LX-500F; Sanso). Flashes at different wavelengths were obtained by passing the light beam through interference filters (λ_{max} with the full bandwidth at half maximal transmittance as follows: 500 nm with 2.6 nm; 600nm with 6.9 nm; 652 nm with 9.0 nm; 676 nm with 9.7 nm) and neutral density filters (Toshiba). Unattenuated light was calibrated by a Digi-Ana Power Meter (PM245; Neoark) that was placed on the microscope stage at the same position as the recorded cells. As described previously (Baylor et al., 1979; Nikonov et al., 2005), the effective collecting area $Ac(\lambda)$ of the mouse rod for a flash of λ nm is given by

$$Ac(\lambda) = 2.303\, f\, \varepsilon_\lambda\, \gamma\, C V_{os} \times 10^{-4}, \qquad (1)$$

where f is a factor allowing for the use of unpolarized light entering the outer segment perpendicular to its axis ($f = 3/4$), ε_λ(M^{-1} cm^{-1}) is the extinction coefficient at λ nm of the pigment in solution, γ is the quantum efficiency of photoisomerization, C (M) is the concentration of the pigment in outer segment, and V_{os} (µm^3) is the individual outer segment volume. The length of outer segments was calculated from digital images of the cells on the light microscope by image analysis software (AquaCosmos 2.5;

Hamamastu Photonics) and its diameter was measured on the electron micrograph. The values of ε_{500} are 40,200 for mouse rhodopsin (Imai et al., 2007) and 43,900 for mouse green, which was calculated based on ε_{510} of mouse green (Onishi et al., 2005) and its absorption spectrum (Fig. 6 B, red trace). The quantum efficiency is $\gamma = 0.67$ for mouse rhodopsin (Dartnall, 1968) and $\gamma = 0.61$ for mouse green (see Results). The total number of rod photoreceptors in mouse retina was estimated as 4.1×10^6 from the product of the total area of the mouse retina (mm^2) and the density of rods per unit area in the retina (rods mm^{-2}); the total area of the mouse retina was estimated as 14.1 mm^2 (Lyubarsky and Pugh, 1996) and the density of rods per unit area in the retina was estimated as 2.9×10^5 rods mm^{-2} provided that the ellipsoid region of inner segment with a diameter of 2.0 µm (Carter-Dawson and LaVail, 1979) was arranged with closest hexagonal packing columns. Since a diameter and length of outer segment was 1.4 and 15 µm for wild-type rod and 1.4 and 6.3 µm for mG/mG rod (TABLE I), V_{os} was 24 µm^3 for wild type and 9.8 µm^3 for mG/mG. Given that the number of rod photoreceptor cells contained in the retina was 4.1×10^6 cells for wild type and the number of cells was the same for the mG/mG retina, C was estimated to be 4.3 mM for wild-type rods and 1.2 mM for mG/mG rods. Thus, the effective collecting area $Ac(500)$ (µm^2) was 0.47 µm^2 for wild-type rods and 0.054 µm^2 for mG/mG rods, respectively.

Amplification Constant

The amplification constant was estimated by fitting the initial portion of the rising phase of the photocurrent response with Eq. 22 of Pugh and Lamb (1993):

$$r(t) = R_{max}\left\{1 - \exp\left[-\tfrac{1}{2} A \Phi\left(t - t_{eff}\right)^2\right]\right\} \text{ for } t > t_{eff}, \qquad (2)$$

where $r(t)$ and R_{max} are the photoresponse and the maximal response, t_{eff} is a combined delay time for all steps, and A is the gain factor for the activation phase of phototransduction, that is, the amplification factor. The combined delay originated from analogue filtering and 20-ms flashes was not corrected. The number of photoisomerizations per rod for λ-nm light Φ is given by

$$\Phi = i\, Ac(\lambda), \qquad (3)$$

where i (photons µm^{-2}) is the flash intensity at λ nm and $Ac(\lambda)$ is the effective collecting area at λ nm given by Eq. 1. The responses evoked by 7–10 intensities for each cell were fit.

Spectral Sensitivities

Spectral sensitivities in single rod cells were determined by dividing the amplitude of the dim flash response (pA) by the given intensity (photons µm^{-2}) at each wavelength. Each dim flash response was averaged from photoresponses elicited by more than 30 times identical flashes.

Noise Analysis

The one-sided power spectral densities were calculated using the Fast Fourier Transform weighted with a Hamming window (Clampfit 8.2 software; Axon Instruments). Power spectra were determined from 25–50 sweeps of 10.24-s-long segments, recorded from cells under each condition. Each current record was filtered at 30 Hz with an eight-pole Bessel low-pass filter and digitized at 400 Hz. Each spectral density was averaged and then smoothed by averaging over neighboring 3 points from 0 to 1 Hz, 5 points from 1 to 6 Hz, 10 points from 6 to 10 Hz, and 20 points above 10 Hz. For noise experiments in darkness, all light paths into the Faraday cage were sealed.

Instrumental Johnson noise level was calculated from the measured electrode resistance and absolute temperature using the

Nyquist Equation, $S(f) = 4kT/\rho$, where k is Boltzmann's constant (1.38×10^{23} J/K), ρ (Ω) is measured electrode resistance, and T (K) is absolute temperature. The measured power spectrum $Sv(f)$ of the dim flash response as a function of frequency f was fit with the equation

$$Sv(f) = Sv(0)\prod_{n=1}^{4}\left[1 + \left(2\pi f / n\alpha\right)^2\right]^{-1}, \qquad (4)$$

where $Sv(0)$ is the zero frequency asymptote (Baylor et al., 1980). For each cell, the value of the rate constant α was determined by fitting the Independence expression with $n = 4$ stages to the dim flash response (Baylor et al., 1980). The rate of thermal activations of visual pigments in rods v_d was then estimated as

$$\nu_d = \frac{Sv(0)}{2(r_p t_i)^2}, \qquad (5)$$

where r_p and t_i are the amplitude and integration time of the single photon response (Baylor et al., 1980). The power spectrum of current fluctuation originated from components downstream from the visual pigments, $Sc(f)$, were fit with the equation as follows

$$Sc(f) = Sc(0)\left[1 + \left(2\pi f / \beta\right)^2\right]^{-2}, \qquad (6)$$

where $Sc(0)$ is the zero frequency asymptote. A product of two Lorentzians with equal half-power frequencies was adopted to empirically fit the continuous noise spectrum in intact toad rods (Baylor et al., 1980).

In the bleaching experiment, the fractional bleaching pigments of the rod, $F(I_s, T_s)$, was estimated as follows

$$F(I_s, T_s) = 1 - \exp[-Ac(500)I_s T_s / P_{tot}],$$

where $Ac(500)$ is the effective collecting area for 500-nm light (μm^2) of the rod, I_s is intensity of a light step (photons $\mu m^{-2}\,s^{-1}$ at 500 nm), T_s is duration of a light step (s), and P_{tot} is the total number of pigment molecules per rod.

We used the two-tailed unpaired Student's t test to determine the significance of difference among the results unless otherwise noted. Experimental data were fit using Levenberg–Marquardt algorithm (IgorPro5.0, WaveMetrics).

RESULTS

Generation of Knock-in Mice Having Cone Pigments in Rod Photoreceptor Cells

The targeting vector was designed to replace the mouse rhodopsin gene with the cDNA sequence of mouse green (Fig. 1 A). Because the mouse green gene located on X chromosomes is up to ~20 kb in length, it seemed difficult to induce homologous recombination with the arm region of the rhodopsin gene. Therefore, we introduced mouse green cDNA (mG) that was followed by the rhodopsin polyadenylation signals (PA) and the neomycin-resistant marker (neo) into the first exon region of the rhodopsin gene. The targeting vector was electroporated into ES cell lines, and one of the 120 ES clones was identified as a homologous recombinant by selection with G418, a neomycin analogue, and Southern blot analysis.

The knock-in mice were generated by blastocyst injection of the ES clones (Fig. 1 B), and it was confirmed that the knock-in mice were viable and fertile.

Replacement of mRNA and Protein for Visual Pigment. To examine whether rhodopsin was successfully replaced with mouse green in the retinas of knock-in mice, we analyzed the expression levels of mRNA and protein for rhodopsin and mouse green. Total RNAs prepared from retinas were analyzed by RT-PCR (Fig. 1 C). RT-PCR products derived from rhodopsin transcripts were detected in wild-type (Rh/Rh) and heterozygous (Rh/mG) retinas but not in homozygous (mG/mG) retinas, whereas RT-PCR products derived from the introduced mouse green transcripts were detected only in Rh/mG and mG/mG retinas. Comparative RT-PCR analysis with Rh/mG retinas showed that the efficacy of transcription of mouse green was ~60% of that of rhodopsin (unpublished data). Western blot analysis with anti-rhodopsin monoclonal antibody (Rhodopsin 1D4) showed that rhodopsin was present in wild-type and heterozygous retinas (Fig. 1 D, top). The intensity of the rhodopsin band in the heterozygous lane was about half that in the wild-type lane, and the rhodopsin band was undetectable in the homozygous lane. On the other hand, in the wild-type lane, we could detect a faint band with anti-mouse green antibody, corresponding to mouse green endogenously expressed in cone cells, while in both Rh/mG and mG/mG lanes much denser bands were detected. (Fig. 1 D, bottom). These results indicated that the replacement of rhodopsin with mouse green was successful at the levels of both mRNA and protein.

Pigment Content in WT and mG/mG Rods. Based on absorption spectroscopy, we estimated the amount of pigments in the retinas of 4-wk-old mice (Table I). The amount of visual pigment (mouse green) per retina in mG/mG mice was 47 pmol, which was 11% of that (rhodopsin) in wild-type mice (410 pmol). On the assumption that each strain of mouse had the same number of rods in its retina, and using the number of 4.1×10^6 cells for wild type (see Materials and Methods), we estimated the number of visual pigments per rod to be 6.1×10^7 molecules in wild-type rods and 7.0×10^6 molecules in mG/mG rods. The photosensitivity at 500 nm of mouse green relative to that of rhodopsin was 0.99 (Fig. 2 A). Thus, the quantum yield of mouse green was estimated to be 0.61 from the relationship that photosensitivity at 500 nm is proportional to the product of the extinction coefficient at 500 nm (ε_{500}) and the quantum yield (γ).

Pigment Content in Rh/mG Mice. Although both rhodopsin and mouse green were coexpressed in heterozygous retinas, the ratio of these visual pigments in Rh/mG retinas can be estimated by means of the different accessibility of these visual pigments to hydroxylamine. Hydroxylamine
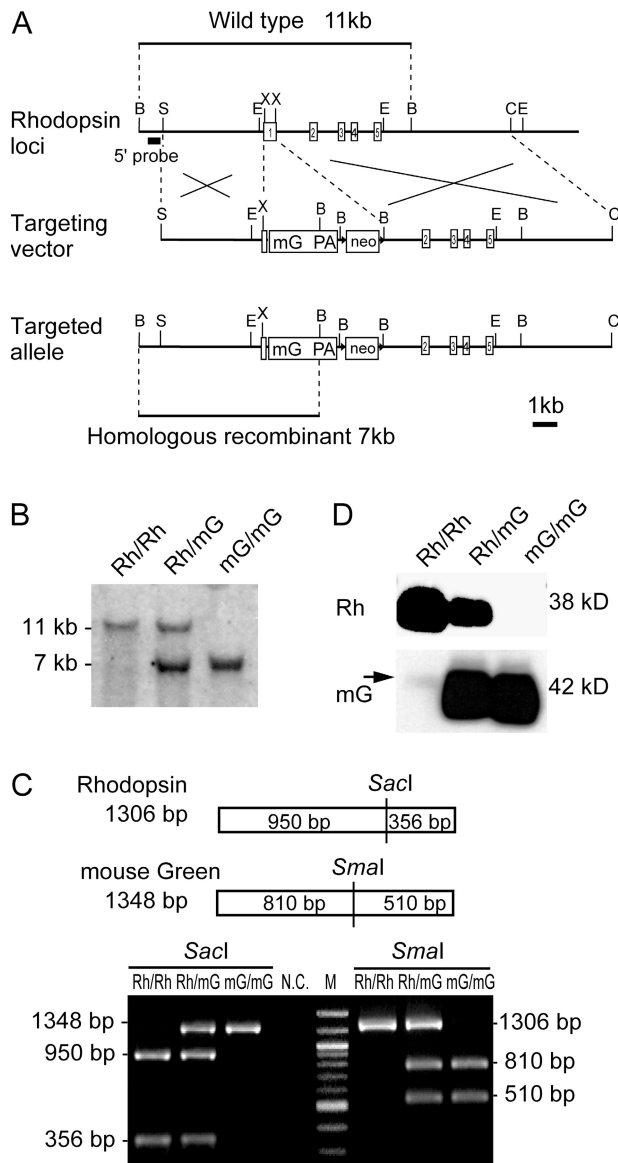
reacts with the retinal in a Schiff base linkage, forming retinal oxime and apoprotein. This reaction rate of loss of cone pigment is substantially faster as compared with that of rhodopsin (Okano et al., 1989; Johnson et al., 1993). Therefore, the heterozygous retinal extracts, which contain both rod and cone pigments, will undergo a biphasic change in the reaction with hydroxylamine. Fig. 2 B shows the time courses of hydroxylamine bleaching in the dark for rhodopsin (open squares), mouse green (red closed circles), and a mixture of rhodopsin and mouse green (open triangles) extracted from wild-type, mG/mG, and Rh/mG retinas, respectively. The time constants of bleaching reactions were 127 h for rhodopsin (open squares) and 1.93 h for mouse green (red closed circles). Based on the time constants of bleaching reactions for each type of visual pigments, the bleaching process of heterozygous retinas (open triangles) was fit with the double-exponential function with the time constants of rhodopsin (127 h) and mouse green (1.93 h). The ratio of the amount of rhodopsin to that of mouse green in Rh/mG retina was estimated to be 90 to 10. This ratio was comparable to the ratio of the amount of rhodopsin in wild-type retinas to the amount of mouse green in mG/mG retinas (9 to 1).

Content of Other Proteins of Transduction. We next estimated the contents of phototransduction proteins other than the visual pigments in the retinas of 3-, 4-, and 6-wk-old mice (Fig. 2 C). The left panel of Fig. 2 C shows the

targeted allele are detected by the 5′ flanking probe shown in A. (C) RT-PCR analysis to verify the replacement of the transcripts. The upper diagram represents the predicted RT-PCR products from rhodopsin and introduced mouse green transcripts. The length of RT-PCR products derived from wild-type and knock-in alleles are 1306 and 1348 bp, respectively. SacI digestion yields 950- and 356-bp fragments of RT-PCR product from rhodopsin transcripts. On the other hand, SmaI digestion yields 810- and 538-bp fragments from introduced mouse green transcripts. In wild-type lanes (Rh/Rh), SacI digestion yielded two fragments of 950 and 356 bp, but SmaI did not. Conversely, in mG/mG lanes, SmaI digestion yielded two fragments of 810 and 510 bp, but SacI digestion did not. In the Rh/mG lanes, both SmaI and SacI digestion yielded two fragments reflecting the presence of both rhodopsin and mouse green transcripts. In the negative control (N.C.) lane, no PCR product was detected from the total RNA sample of mG/mG retina, ensuring that PCR products observed here were derived from mRNA. *M* represents DNA size marker (from top to bottom: 1,517, 1,200, 1,000, 900, 800, 700, 600, 500, 400, and 300 bp). (D) Western blots using the antibodies against rhodopsin (top panel) and mouse green (bottom panel). Rhodopsin was detected by rhodopsin 1D4 antibody at 38-kD position, which showed the genotype-dependent expression. A faint band was detected for mouse green endogenously expressed in cone photoreceptors at 42 kD in the Rh/Rh lane (arrow), whereas in the Rh/mG and mG/mG lanes intense bands from the recombinant mouse green were detected at the same position. An equal amount of retinal lysate (0.003% of a retina for rhodopsin 1D4 antibody and 1.3% of a retina for anti-mouse green antibody) was loaded in each lane.

Figure 1. Generation of mouse green cone pigment knock-in mice. (A) Targeting strategy to generate mouse green knock-in mice. The restriction maps of the mouse rhodopsin genomic locus (top), the targeting vector containing mouse green opsin cDNA (mG) (middle) and the predicted genomic structure of the knock-in allele after homologous recombination (bottom). The five exons of the rhodopsin gene are shown as the open rectangles (1–5). The crossed broken lines indicate the areas of homology between the wild-type rhodopsin locus and the targeting vector. The chimeric intron is inserted into XhoI site in the 5′ untranslated region of rhodopsin gene. The translation initiation codon of mouse green opsin cDNA sequence (mG) was placed at the same position as that of mouse rhodopsin gene. The subsequent PA represents the rhodopsin polyadenylation signals. The phosphoglycerate kinase driven neomycin resistance gene (neo) is flanked by 34-bp *lox*P sequences (triangles). Digestions with BamHI distinguish the homologous recombinant fragments (7 kb) from the wild-type fragments (11 kb). Restriction sites: B, BamHI; C, ClaI; E, EcoRI; S, SpeI; X, XhoI. (B) Southern blots of BamHI-digested mouse tail genomic DNA from wild-type (Rh/Rh), heterozygous (Rh/mG), and homozygous (mG/mG) mice. The 11-kb fragments from wild-type allele and 7-kb fragments from

TABLE I

Parameters of Morphology and Single Cell Responses by Suction Electrode

	Wild type	mG/mG
Morphological parameters		
OS length (μm)	15 ± 0.5 (10)	6.3 ± 0.3 (12)[b]
OS diameter (μm)	1.4 ± 0.1 (7)	1.4 ± 0.1 (6)
Pigment content (pmol/retina)	410 ± 35 (4)	47 ± 3 (6)[b]
Single cell recordings		
r_{max} (pA)	8.1 ± 0.3 (22)	5.9 ± 0.5 (14)[b]
I_0 (photons μm^{-2})	20.7 ± 0.8 (22)	725 ± 50 (14)[b]
$I_0Ac(500)$ (R*, photoisomerizations/rod)	9.7 ± 0.4 (22)	39 ± 3 (14)[b]
Integration time (ms)	233 ± 9 (18)	191 ± 9 (14)[a]
Time to peak (ms)	147 ± 2 (18)	139 ± 5 (14)
Single photon response (pA)	0.66 ± 0.05 (17)	0.16 ± 0.02 (13)[b]
A_0 (s^{-2})	25 ± 1 (13)	7.0 ± 0.7 (6)[b]

Values are means ± SEM. The number used to determine each parameter is given in parentheses. r_{max} is saturating photoresponse amplitude. I_0 is flash intensity at 500 nm, which gives the half maximal response. Time to peak and integration time were estimated from responses whose amplitude are $<0.2r_{max}$ and within the linear range. Integration time is the area of the dim flash response divided by its peak amplitude. The amplitude of the single photon response was obtained from ensemble variance-to-mean ratio of the dim flash response. A_0 is a gain factor for the rising phase of phototransduction cascade determined by fitting the equation of Pugh and Lamb (1993) to multiple responses of each cell.
[a]Difference from wild-type rods being statistically significant, P < 0.05.
[b]Difference from wild-type rods being statistically significant, P < 0.005.

blotting patterns of various transduction proteins in the retinas of 4-wk-old wild-type (Rh/Rh), Rh/mG, and mG/mG mice. The intensities of all bands in mG/mG retinas, especially that of the transducin α-subunit, were faint relative to those in wild-type and Rh/mG retinas. It should be noted that age-dependent alteration was not observed at least during a period of 3–6 wk. The amounts of proteins in mG/mG retinas relative to those of wild-type retinas were quantified and the results are shown in the right panel of Fig. 2 C. The amount of transducin α-subunit in mG/mG retinas was ∼0.2-fold of wild type, whereas those of the other proteins were 0.4–0.5-fold of wild type. From morphological studies, the total surface area of disc membrane or a surface area of plasma membrane of rod outer segment of mG/mG retinas was estimated to be 0.4-fold of wild type. Thus assuming that the same numbers of rod photoreceptor cells were present in wild-type and mG/mG retinas, the concentration, defined as the density per unit area of membrane, of transducin α-subunit in mG/mG rod was estimated to be half of wild type, whereas the concentrations of other phototransduction proteins in mG/mG rod were similar to those in wild type. In Rh/mG retinas, the concentration of transducin was found to be ∼0.6-fold lower than that in wild-type retinas, but those of other proteins were similar to those in wild-type retinas.

Light Microscopy. The retinal structure of 3-wk-old mice was first investigated by light microscopy. The structure appeared to be normal in both Rh/mG and mG/Mg mice (Fig. 3), although the length of the ROS in homozygous mice was about half that in wild type. From careful measurements of cell dimension, we estimated that

the outer segment length was 15 μm for wild-type rods but only 6.3 μm for mG/mG rods; i.e., ∼40% of wild type (Table I).

Immunohistochemistry. Immunohistochemical analysis showed that monoclonal antibody against rhodopsin uniformly stained the ROS layer of wild-type and Rh/mG retinas but not that of mG/mG retinas (Fig. 3, B, F, and J). On the other hand, mouse green, which is endogenously expressed in cones, was detected only in the cone outer segments of wild-type retinas (Fig. 3 C). In Rh/mG retinas, colocalization of rhodopsin and mouse green in the ROS layer was observed (Fig. 3 H). ROS of the mG/mG retinas were stained with the antibody against mouse green (Fig. 3, G and K). Therefore, the expression pattern of mouse green from integrated allele was apparently under the endogenous regulatory control, and mouse green was successfully transported to the ROS.

Electron Microscopy. The structure of the ROS was further examined by electron microscopy, which showed that the outer segments appeared to be similar in structure between wild-type and Rh/mG mice at 3 wk of age (Fig. 3, M and N). Under careful observation, however, the discs in the ROS of mG/mG mice were well stacked and maintained normal size in the basal region but became gradually more disorganized toward the apical region with formation of vesicles (Fig. 3 O). The neural retina of mG/mG mice seemed to degenerate slowly at 3 wk of age, but in the retinas of 7-wk-old mice, the structure of the outer segments had severely degenerated (Fig. 3 P). It is likely that the level of expression of mouse
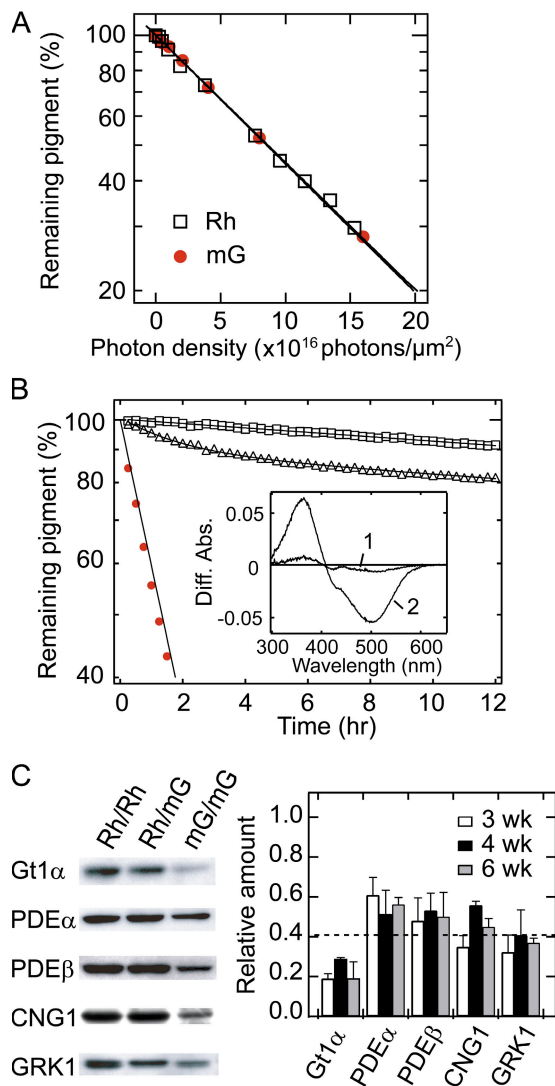
green pigment was too low to maintain the stability of the outer segments disks. The same reasoning could be applied to the shortening of the ROS in 3-wk-old mG/mG mice. Judging from the morphological and biochemical observations described above, we decided to use 3-wk-old mice for electrophysiological experiments, to minimize the effect of degeneration.

Transducin Activation. We examined transducin activations by mouse rhodopsin or mouse green expressed in ROS membrane. Fig. 4 shows that mouse green can activate transducin at 0°C with an efficiency similar to that of wild-type rhodopsin. These results are in good agreement with previous reports (Fukada et al., 1989; Imai et al., 1997; Starace and Knox, 1997). We also measured the efficiency of transducin activation by mouse green at 37°C (Fig. 4, inset). Although the results showed that the initial rate of activation by mouse green was about half the rate of activation by wild-type rhodopsin, it appeared that the time resolution of the GTPγS binding assay might not be sufficient for monitoring the rapid activation of transducin by cone visual pigments.

Photoresponses from Single-Cell Recordings in Green Cone Pigment Knock-in Mice

To examine the responses of knock-in rods in detail, we recorded with a suction pipette the photoresponses from individual rods of 3-wk-old mice. Fig. 5 A shows typical responses recorded from rods of wild-type and mG/mG mice. Response families for a series of flash strength at 500 nm were qualitatively similar between wild-type and mG/mG rods, although the maximum amplitude was lower and the integration time was slightly faster in mG/mG rods (Table I).

Sensitivity. The half-saturating intensity at 500 nm, I_o, was ~35-fold higher in mG/mG rods than in wild-type

Figure 2. Expression of the functional proteins in the knock-in mice. (A) Photosensitivity measurements of rhodopsin (open squares) and mouse green (red closed circles) at 500 nm. The amount of residual pigment was plotted on a logarithmic scale against the numbers of incident photons. By comparing the bleaching rate (photons^{-1} μm^2) of the fitted exponential curves, which was $(8.0 \pm 0.3) \times 10^{-18}$ for rhodopsin and $(7.9 \pm 0.3) \times 10^{-18}$ for mouse green, the ratio of the photosensitivity at 500 nm of mouse green to that of rhodopsin was estimated to be 0.99. Errors indicate 95% confidence interval of the parameters. (B) Estimation of the ratio of the amount of rhodopsin and mouse green in Rh/mG retinas. The visual pigments extracted from the retinas of wild-type (open squares), Rh/mG (open triangles), and mG/mG (red closed circles) mice were subjected to the sensitivity measurements in 200 mM neutralized hydroxylamine at 20°C. The remaining visual pigments (%) were plotted as a function of the incubation time (h). The bleaching processes of rhodopsin (open squares) and mouse green (red closed circles) were fit with single-exponential functions with time constants of 127 h and 1.93 h, respectively. The bleaching process of a mixture of rhodopsin and mouse green (open triangle) in heterozygous retinas monitored at 500 nm was fit with a double-exponential function with time constants of 127 h (89%) and 1.93 h (11%). After correcting for the different molecular extinction coefficient at 500 nm, the proportion of rhodopsin to mouse green

was estimated to be 90 to 10. (Inset) The difference absorption spectra of the Rh/mG retinal extract. Curve 1 is the difference spectrum calculated by subtracting the spectrum immediately after adding hydroxylamine from that 4 h after incubation in the presence of hydroxylamine. Curve 2 is the difference spectrum calculated by subtracting the spectrum 4 h after incubation in the presence of neutralized hydroxylamine from that after complete bleaching by irradiation with >500-nm light. (C) Comparison of the phototransduction proteins in retinal homogenates. (Left) Western blots of wild-type (Rh/Rh), heterozygous (Rh/mG), and homozygous (mG/mG) mice. In each lane, 1.3% homogenate of one retina at 4-wk-old mice were electrophoresed for blotting. (Right) Protein expression levels in the retinas of homozygous (mG/mG) mice relative to those of wild-type mice. Mice of 3, 4, and 6 wk old were subjected to the experiments. The horizontal broken line indicates the ratio of total surface area of outer segment of mG/mG rod relative to that of wild-type one. The values from three to four experiments were averaged with SEM bars. Gt1α, rod transducin α subunit; PDEα, phosphodiesterase α subunit; PDEβ, phosphodiesterase β subunit; CNG1, cyclic nucleotide-gated channel 1; GRK1, G-protein receptor kinase 1.
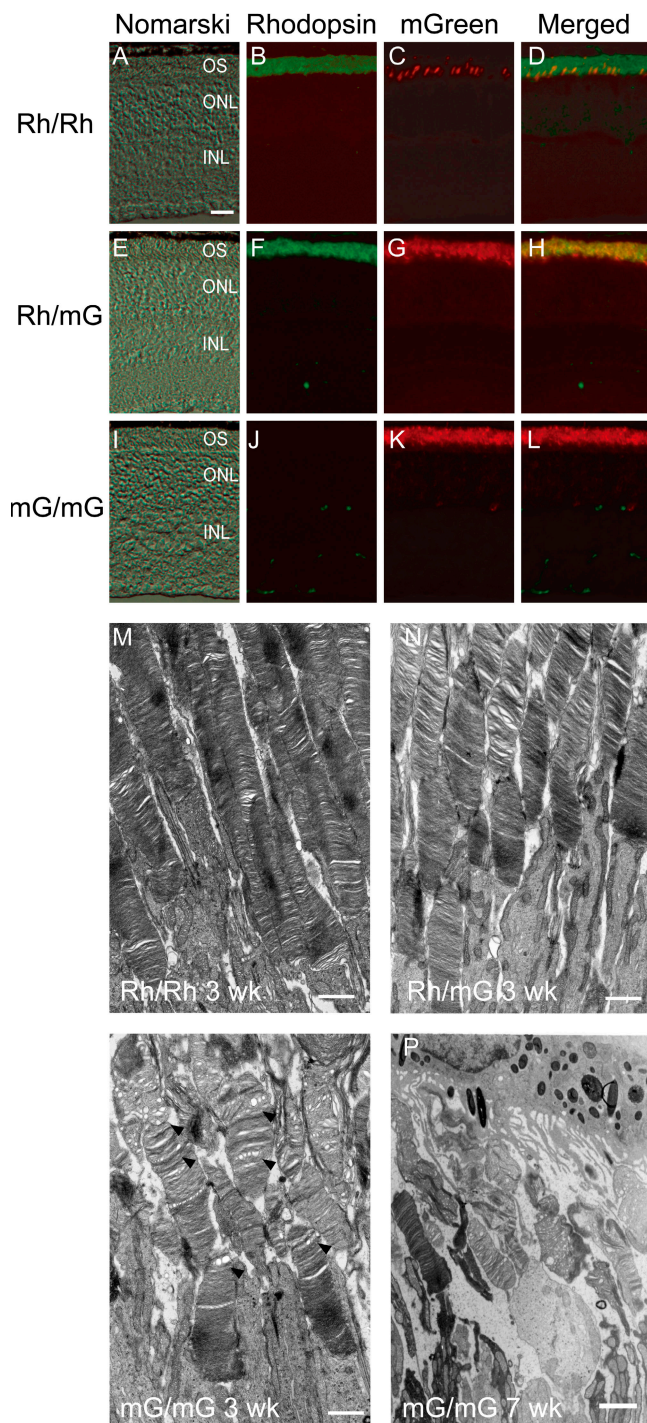
Figure 3. Morphology and histological expression patterns of rhodopsin and mouse green. Retinal sections of 3-wk-old wild-type, heterozygous, and homozygous mice are shown in A–D, E–H, and I–L. (A, E, and I) Nomarski images. (B, F, and J) Stained for rhodopsin (green). (C, G, and K) Stained for mouse green (red). (D, H, and L) Merged. OS, outer segments; ONL, outer nuclear layer; OPL, outer plexiform layer; INL, inner nuclear layer. (M–P) Electron micrographs of the photoreceptors of 3-wk-old (M) wild-type, (N) heterozygous, and (O) homozygous mice. Wild-type discs stacked tightly within the ROS and were oriented perpendicular to the long axis of the ROS. Heterozygous (Rh/mG) discs appeared to be normal. Homozygous (mG/mG) discs of normal size stacked neatly at the basal region of outer segments but the distal discs occasionally formed vesicle-like structures (arrowheads). (P) Photoreceptors of 7-wk-old homozygous (mG/mG) mouse. Magnification bars are 20 μm (A–L) and 1 μm (M–P).

rods (Table I), comparable to the 32-fold difference estimated from electroretinogram experiments (unpublished data). This large difference in sensitivity stems in part from the different effective collecting area of the cells (as a result of the different pigment content), and when recalculated in terms of the numbers of photoisomerizations the difference is much smaller. Given the estimates of effective collecting areas at 500 nm, $Ac(500)$, of 0.47 μm² for wild-type and 0.054 μm² for mG/mG rods (see Materials and Methods), we calculated the number of photoisomerizations required to half-saturate the response to be 9.7 R* for wild-type rods and 39 R* for mG/mG rods (Fig. 5 B and Table I); thus, when expressed in terms of photoisomerizations, the mG/mG rods are less sensitive by a factor of only 4.0.

Single-Photon Responses. We stimulated rods with at least 30 consecutive identical dim flashes and estimated the amplitude of the single-photon response from the ensemble variance-to-mean ratio of the response amplitude based on the assumption of Poisson statistics (Baylor et al., 1979). The mean amplitude of the single-photon response from 13 mG/mG rods was 0.16 pA, which was 4.1-fold smaller than that from 17 wild-type rods (0.66 pA). The difference in amplitude of the single-photon response between wild-type and mG/mG rods should be compared with each other after expressing their single-photon responses as the fractional circulating currents. The amplitude of single-photon response in wild-type rods was 8.1% of the circulating current, while that in mG/mG rods was 2.7%. Thus the fractional circulating current in wild-type rods is three-fold larger than that in mG/mG rods. Therefore, a large part of the 4.0-fold difference in the quantal sensitivity for 500-nm light ($I_oAc(500)$) can be attributed to the difference in amplitude of the single-photon response. The integration time of dim flash responses for homozygous rods was 1.2-fold shorter than for wild-type rods, whereas the time-to-peak in mG/mG rods was similar to that in wild-type rods (Table I), suggesting that the shorter integration time results from an accelerated recovery phase. Since the time-to-peak of mG/mG rods was similar to that of wild-type rods, the lower sensitivity and the smaller amplitude of single-photon responses of mG/mG rods could be attributed to a reduction in the rising phase of the response, which related to the gain of the phototransduction cascade.

Amplification Constant. The gain of phototransduction cascade can be evaluated as the amplification constant by fitting the rising phases of the photoresponses with
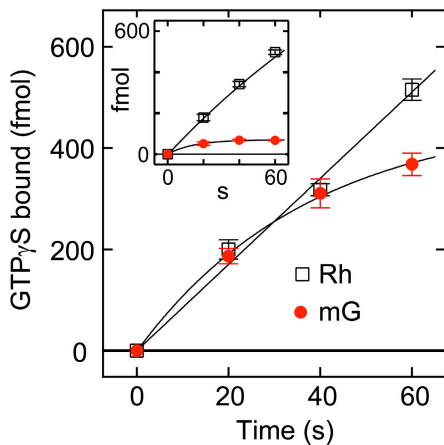
Figure 4. Comparison of G-protein activation by rhodopsin (open squares) and mouse green (red filled circles) in ROS membranes at 0°C. The amount of light-dependent GTPγS-bound transducin was plotted as a function of incubation time after irradiation. The solid curves indicate the results by fitting a linear function for the data of rhodopsin and a single-exponential function for the data of mouse green. The initial rate of GTPγS bound (fmol s^{-1}) was 10 ± 0.4 for rhodopsin ($n = 4$) and 13 $\pm$ 1.3 for mouse green ($n = 4$; P > 0.05). (Inset) Time courses of G-protein activation efficiencies of rhodopsin (open squares) and mouse green (red filled circles) in ROS membrane at 37°C. The initial rate of GTPγS bound (fmol s^{-1}) was 8.3 ± 0.3 for rhodopsin ($n = 4$) and 4.6 ± 0.7 for mouse green (n = 3; P < 0.05). Error bars indicate SEM.

Eq. 2. This equation is applicable only during the initial phase of the responses before inactivation reactions set in, and hence allows quantitative comparison of activation in each type of the cell. In the application of the amplification constants for the rising phase, it is assumed that the involvement of any inactivation step is neglected. It should be noted that we are unable to fully exclude the possibility that rapid intrinsic turn-off of the active state of mouse green occurs during the rising phase of the photoresponse (see Discussion).

The mean amplification constant from 13 wild-type rods was 25 s^{-2} (Fig. 5 C), which is relatively higher than those previously reported (13.6 s^{-2}, Calvert et al., 2001; 8.3 s^{-2}, Nikonov et al., 2006). The discrepancy might arise from the age-related variations such as the smaller cytoplasmic volume of the outer segment or higher concentrations of transduction components in young mice. The mean amplification constant from six mG/mG rods was 7.0 s^{-2} (Fig. 5 C), which is 3.6-fold smaller than that of wild-type rods.

In terms of the theory derived by Pugh and Lamb (1993), the difference in the amplification constant between that for control rods and that for rods containing mouse green can be explained by two factors: the outer segment volume and the rate of transduction activation by activated photopigment; however, this latter factor is likely to be affected by the concentration of transducin in the disc membranes. The amplification constant is predicted to be inversely proportional to the outer segment volume because a given number of activated molecules can change the cytoplasmic concentration of cyclic GMP more rapidly. Hence, our finding that the outer segment volume of mG/mG rods is only 42% that of wild-type rods would, in itself, predict an elevation of 2.4-fold in amplification constant. Hence the observation of an amplification constant that is lower by a factor of 3.6-fold in mG/mG rods would indicate that the rate of transducin activation is a factor of 8.6-fold lower in mG/mG rods. However, it would be expected that the 0.5-fold lower concentration of transducin in the membrane would contribute to this difference, so that the efficacy of the activated mouse green pigment molecule in activating transducin may only be a factor of 4.3-fold lower than the corresponding efficacy of activated rhodopsin.

Comparison of Photoresponses Evoked by E122Q Rhodopsin and Mouse Green in Single Rod Photoreceptor Cells

As mentioned above, comparison of the electrophysiological responses between wild-type and mG/mG rods showed that the amplitude of photoresponse evoked by mouse green was 3–4-fold lower than that evoked by rhodopsin. This value was derived both from single-photon responses and from sensitivity measurements after correction for the differences in morphology and in concentrations of visual pigment and transduction proteins between wild-type and mG/mG rods. Also, other factors, such as lower pigment concentrations in the disk membranes, may affect the amplification constant (Calvert et al., 2001). To exclude unavoidable uncertainty arising from such corrections, we attempted to evaluate photoresponses produced from rhodopsin and mouse green under identical conditions, using heterozygous mice whose rods contain both of these pigments. However, the spectral sensitivities of rhodopsin and mouse green (with λ_{max} values at 502 and 510 nm, respectively), were so similar that it was difficult to selectively activate one type of these pigments. Therefore, we prepared a heterozygous (Rh^{EQ}/mG) mouse, with rods containing mouse green and E122Q rhodopsin. E122Q rhodopsin exhibits an absorption maximum ($\lambda_{max} = 487$ nm) that is blue shifted ~23 nm from the peak for mouse green but generates photoresponses similar to that of wild-type rhodopsin (Imai et al., 2007).

Pigment Content in Rh^{EQ}/mG Mice. We estimated the ratio of the concentration of E122Q rhodopsin to that of mouse green present in heterozygous (Rh^{EQ}/mG) rods as 91 to 9, determined by the same method used for the Rh/mG mice (Fig. 6 A). This ratio was almost the same as for wild-type rhodopsin and mouse green in Rh/mG rods (see above).
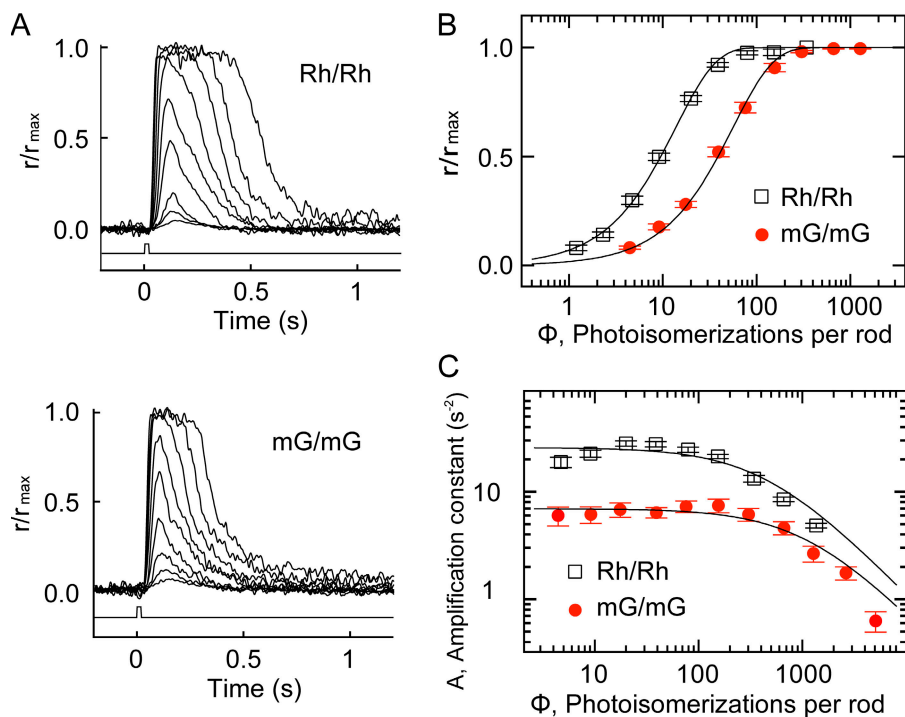
Figure 5. Single-cell recordings of wild-type (Rh/Rh) and homozygous (mG/mG) rods. (A) Normalized flash responses of the wild-type (top) and the mG/mG (bottom) rods to increasing 500-nm flash strength delivered at time 0 with 20 ms duration. Each trace is the averaged responses from multiple flash trials. Flash monitor is shown by bottom trace in each panel. Flash intensities were 2.5, 4.9, 10, 19, 43, 82, 170, 330, and 730 photons μm^{-2} in the wild-type rod, while 43, 82, 170, 330, 730, 1.4×10^3, 2.9×10^3, 5.6×10^3, and 1.2×10^4 photons μm^{-2} in the mG/mG rod. The maximal responses were 9.4 pA for the wild-type rod and 8.4 pA for the mG/mG rod. (B) Normalized peak responses plotted as a function of photoisomerizations per rod. Responses of wild-type (open squares; $n = 22$) and mG/mG (red filled circles; $n = 14$) rods were fitted with: $r/r_{max} = 1 - exp(-k'\Phi)$, where Φ is photoisomerizations defined as Eq. 3. $In(2)/k'$ provides photoisomerizations giving the half-saturating response. Mean half-saturating photoisomerizations collected from 22 wild-type and 14 mG/mG rods were 9.7 R* and 39 R*, respectively. (C) Amplification constants as a function of photoisomerizations per flash. Each point of wild-type (open squares; $n = 13$) or mG/mG (red filled circles; $n = 6$) rods is the mean value of A, which was determined by fitting with Eq. 2 to the rising phase of the normalized response. Amplification constant, A_0, of each cell was estimated by fitting with: $A = A_0/(1 + \Phi/\Phi_0)$, where A_0 is the constant value of A at lower intensities and Φ_0 is the photoisomerizations at which A declines to the half maximum. The mean values of A_0 were 25 s^{-2} from 13 wild-type rods and 7.0 s^{-2} from six mG/mG rods. Error bars indicate SEM.

500-nm Light. The photosensitivity of E122Q rhodopsin at 500 nm was also determined by the previously described method, giving a value of 0.93-fold that of mouse green (Fig. 6 B, inset). Based on the effective collecting area of each type of pigments for 500-nm light, Ac(500) (proportional to the product of the photosensitivity at 500 nm, $\varepsilon_{500}\gamma$, and the pigment concentration, C), we calculated the proportion of pigment photoactivated by 500-nm light in Rh^{EQ}/mG rods as 90% E122Q rhodopsin with the remainder being mouse green.

Other Wavelengths. We then estimated the percentages of E122Q rhodopsin and mouse green photoactivated by 600-, 652-, and 676-nm lights in Rh^{EQ}/mG rods. Using single cell recordings, we measured the relative spectral sensitivities of E122Q rhodopsin from 10 Rh^{EQ}/Rh^{EQ} rods and those of mouse green from 11 mG/mG rods (Fig. 6 B and Table II). Because we measured the spectral sensitivities by using the respective homozygous mice, these should be identical with the absorption spectra of E122Q rhodopsin and mouse green, respectively, if the quantum yields of these pigments are wavelength independent (Hurley et al., 1977), although we acknowledge that it is generally accepted that the quantum yields of visual pigments is slightly wavelength dependent. In fact, the spectral sensitivities were found to be superimposable on the absorption spectra of E122Q

rhodopsin and mouse green, when the magnitudes were normalized at 500 nm (Fig. 6 B). The spectral sensitivities and absorption spectrum of E122Q rhodopsin were well fit with the spectral template (broken curve) reported by Govardovskii et al. (2000), whereas some deviation was apparent in the case of mouse green. This might be due to the difference in spectral shape between rhodopsin and long wavelength–sensitive cone visual pigments (Okano et al., 1989). From the ratio of each visual pigments photoactivated at 500 nm in Rh^{EQ}/mG rods and the relative spectral sensitivities of homozygous rods obtained in single cell recordings (Table II), the percentages of the pigments photoactivated in Rh^{EQ}/mG rods at the corresponding wavelengths could be determined. Thus, the percentages of E122Q rhodopsin photoactivated at 500, 600, 652, and 676 nm were estimated to be 90, 31, 16, and 12% of the total photoisomerizations, respectively (Rh^{EQ}:mG in Table III). Importantly, the response evoked by 500-nm light is expected to be mainly from E122Q rhodopsin, and that evoked by the longer wavelengths is expected to be mostly from mouse green.

Photoresponses at Different Wavelengths. We then recorded a set of responses from a Rh^{EQ}/mG rod using dim flash illuminations at wavelengths of 500, 600, 652, and 676 nm (Table III). We then recorded the responses
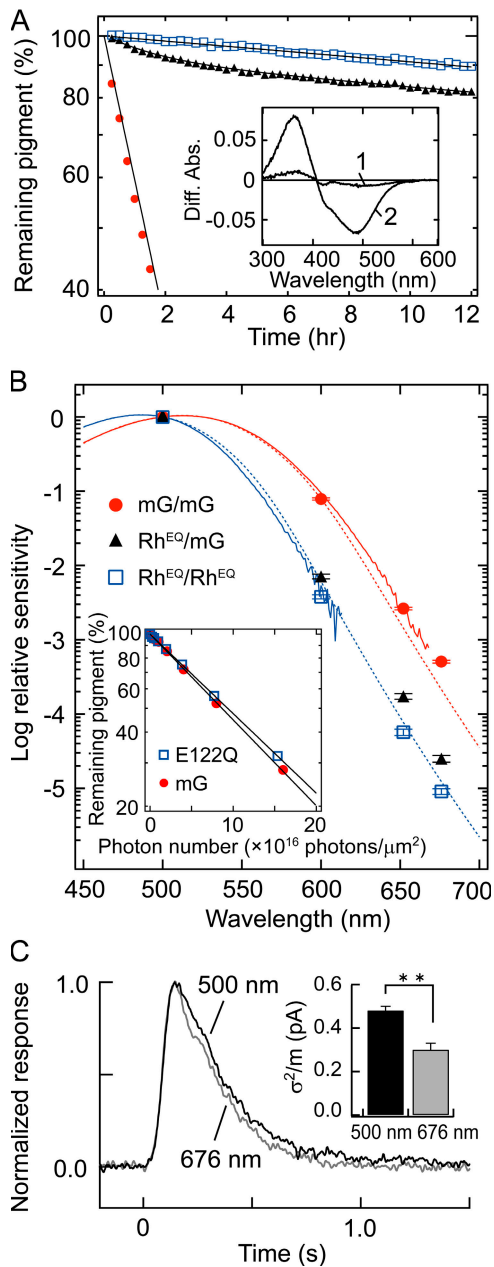
Figure 6. Characterization of the E122Q rhodopsin and mouse green in the heterozygous (Rh^{EQ}/mG) rods. (A) Estimation of the ratio of the amount of E122Q rhodopsin and mouse green in Rh^{EQ}/mG retinas. The pigments extracted from the retinas of Rh^{EQ}/Rh^{EQ} (blue open squares), Rh^{EQ}/mG (closed triangle), and mG/mG (red closed circles) mice were subjected to the sensitivity measurements in 200 mM neutralized hydroxylamine at 20°C. The remaining visual pigments (%) were plotted as a function of the incubation time (h). The bleaching processes of E122Q rhodopsin and mouse green were fit with single-exponential functions with time constants of 107 h and 1.93 h, respectively. The bleaching process of a mixture of E122Q rhodopsin and mouse green from heterozygous mice was monitored at 498 nm (isosbestic point of E122Q rhodopsin and mouse green) and then fit with a double-exponential function with time constants of 107 h (91%) and 1.93 h (9%). The proportion of E122Q rhodopsin to mouse green was estimated to be 91 to 9. (Inset) The difference absorption spectra of the Rh^{EQ}/mG retinal extract. Curve 1 is the difference spectrum calculated by subtracting the spectrum

evoked by the 500-nm flash again The times-to-peak of the responses were not significantly different at the different illumination wavelengths, but the integration times obtained with the longer wavelength flashes were slightly shorter than that obtained with the 500-nm flash (Fig. 6 C; Table III). These results are consistent with the facts that the time-to-peak of mG/mG rods was similar to that of wild-type rods and that the integration time was slightly shorter in mG/mG rods than in wild-type rods.

As previously described, the percentage of photoactivated E122Q rhodopsin was expected to be small when the rod was irradiated with long wavelength flashes. Interestingly, the ratio of the ensemble variance-to-mean decreased at longer wavelength (Table III; Fig. 6 C, inset). This was not due to any change in physiological state of the cells because the 500-nm photoresponses did not change through the experiment (c.f. the value of 500 nm pre and that of 500 nm post in Table III). The ensemble variance-to-mean ratio obtained in the present study does not represent the amplitude of the elementary response of either mouse green or E122Q rhodopsin because irradiation at any wavelength induces photoreactions of both mouse green and E122Q

immediately after adding hydroxylamine from that 4 h after incubation in the presence of hydroxylamine. Curve 2 is the difference spectrum calculated by subtracting the spectrum 4 h after incubation in the presence of neutralized hydroxylamine from that after complete bleaching by irradiation with >500-nm light. (B) Spectral sensitivities at 600, 652, and 676 nm relative to 500 nm. Mean spectral sensitivities at these wavelengths relative to that at 500 nm, which were obtained from Rh^{EQ}/Rh^{EQ} (blue open squares; $n = 10$), mG/mG (red closed circles; $n = 11$), and Rh^{EQ}/mG (closed triangles; $n = 14$) rods by suction electrode recordings, were plotted against wavelength. The values are described in Table II. The solid curves are the absorption spectra (at 20°C) of E122Q rhodopsin (blue curve; $\lambda_{max} = 487$ nm) and mouse green (red curve; $\lambda_{max} = 510$ nm), which are normalized at 500 nm. The broken curves are the template spectra of visual pigments whose λ_{max} are located at 487 nm (blue broken curve) and 510 nm (red broken curve). These template spectra were described previously (Govardovskii et al., 2000). (Inset) Photosensitivity measurements of E122Q rhodopsin (blue open squares) and mouse green (red closed circles) at 500 nm. The amounts of residual pigment were plotted on a logarithmic scale against the numbers of incident photons. By comparing the bleaching rate (photons^{-1} μm^2) of the fitted exponential curves, which was $(7.3 \pm 0.2) \times 10^{-18}$ for E122Q rhodopsin and $(7.9 \pm 0.3) \times 10^{-18}$ for mouse green, the ratio of photosensitivity at 500 nm of E122Q rhodopsin to that of mouse green was estimated to be 0.93. Errors indicate 95% confidence interval of the parameters. (C) The grand mean of dim flash response kinetics from 14 heterozygous (Rh^{EQ}/mG) rods evoked by consecutive identical flashes with 500 nm (black trace) and 676 nm (gray trace). These traces are normalized at peak response. (Inset) The variance-to-mean ratios of the responses evoked by 500-nm (black bar) and 676-nm (gray bar) flashes. These values are the averages from 14 Rh^{EQ}/mG rods. The difference in the ensemble variance-to-mean ratio is significant between 500-nm and 676-nm light (P < 0.005; two-tailed paired Student's t test). Error bars indicate SEM.

TABLE II

Relative Spectral Sensitivities to 500-nm light

	600 nm	652 nm	676 nm	Average
Rh^{EQ}/Rh^{EQ} ($n = 10$)	$(3.79 \pm 0.24) \times 10^{-3}$	$(5.71 \pm 0.56) \times 10^{-5}$	$(9.05 \pm 0.81) \times 10^{-6}$	
mG/mG ($n = 11$)	$(7.86 \pm 0.28) \times 10^{-2}$	$(2.63 \pm 0.10) \times 10^{-3}$	$(5.09 \pm 0.22) \times 10^{-4}$	
Rh^{EQ}/mG ($n = 14$)	$(7.12 \pm 0.52) \times 10^{-3}$	$(1.73 \pm 0.15) \times 10^{-4}$	$(2.51 \pm 0.27) \times 10^{-5}$	
g_{mG}/g_{EQ} ($n = 14$)	0.42 ± 0.07	0.44 ± 0.06	0.30 ± 0.05	0.39 ± 0.05

Values are means ± SEM. Sensitivities at 600, 652, and 676 nm relative to that at 500 nm were calculated from the data obtained by single cell recordings. Spectral sensitivities (pA photons^{-1} μm^2) at each wavelength (500, 600, 652, and 676 nm) were estimated by dividing the amplitude of the dim flash response (pA) by the flash intensity (photons μm^{-2}). Relative spectral sensitivites to 500-nm light were calculated by dividing flash sensitivities at each wavelength (600, 652, and 676 nm) by the flash sensitivity at 500 nm. g_{mG}/g_{EQ} represents the ratio of the amplitude of the elementary response of mouse green to that of E122Q rhodopsin, which was calculated from Eq. 9.

rhodopsin. However, these results strongly suggest that the amplitude of the elementary response generated by mouse green is significantly smaller than that generated by E122Q rhodopsin.

Calculation of the Elementary Response Elicited by Different Wavelengths. To compare the amplitude of the elementary responses derived from mouse green and E122Q rhodopsin, we performed the following calculations. The amplitude of dim flash response, if it does not exceed 20% of the maximal response, is proportional to the flash intensity (Field and Rieke, 2002). Therefore, the flash sensitivity of heterozygous (Rh^{EQ}/mG) rods at λ_0 nm, $S_{df}^{EQ/mG}(\lambda_0)$, is obtained by the following equation:

$$S_{df}^{EQ/mG}(\lambda_0) = \left(\Phi^{EQ} g_{EQ} + \Phi^{mG} g_{mG}\right)/i$$
$$= A_c^{EQ}(\lambda_0) g_{EQ} + A_c^{mG}(\lambda_0) g_{mG}, \quad (7)$$

where Φ^{EQ} and Φ^{mG} represent the mean number of photoisomerizations of E122Q rhodopsin and mouse green in a Rh^{EQ}/mG rod evoked by a dim flash of intensity i at λ_0 nm, respectively. $A_c^{EQ}(\lambda_0)$ and $A_c^{mG}(\lambda_0)$ represent the effective collecting area at λ_0 nm in Rh^{EQ}/mG rods for E122Q rhodopsin and that for mouse green, respectively.

g_{EQ} and g_{mG} are the peak amplitude of the elementary responses produced by a single photoisomerization of E122Q rhodopsin and mouse green, respectively.

In a similar way, the sensitivity of Rh^{EQ}/mG rods at λ_1 nm, $S_{df}^{EQ/mG}(\lambda_1)$, is represented as follows:

$$S_{df}^{EQ/mG}(\lambda_1) = A_c^{EQ}(\lambda_1)g_{EQ} + A_c^{mG}(\lambda_1)g_{mG}, \quad (8)$$

where $A_c^{EQ}(\lambda_1)$ and $A_c^{mG}(\lambda_1)$ represent the effective collecting areas at λ_1 nm in Rh^{EQ}/mG rods of E122Q rhodopsin and mouse green, respectively.

From Eqs. 1, 7, and 8, the ratio of the amplitude of the elementary response of mouse green relative to that of E122Q rhodopsin is derived as follows:

$$\frac{g_{mG}}{g_{EQ}} = \frac{S_{df}^{EQ/mG}(\lambda_1)/S_{df}^{EQ/mG}(\lambda_0) - \varepsilon_{\lambda_1}^{EQ}/\varepsilon_{\lambda_0}^{EQ}}{\varepsilon_{\lambda_1}^{mG}/\varepsilon_{\lambda_0}^{mG} - S_{df}^{EQ/mG}(\lambda_1)/S_{df}^{EQ/mG}(\lambda_0)} \times \frac{\varepsilon_{\lambda_0}^{EQ}\gamma^{EQ}}{\varepsilon_{\lambda_0}^{mG}\gamma^{mG}} \times \frac{C^{EQ}}{C^{mG}}, \quad (9)$$

where $\varepsilon_{\lambda_1}^{EQ}/\varepsilon_{\lambda_0}^{EQ}$ and $\varepsilon_{\lambda_1}^{mG}/\varepsilon_{\lambda_0}^{mG}$ are the extinction coefficient at λ_1 nm relative to that at λ_0 nm of E122Q rhodopsin and mouse green, respectively. $S_{df}^{EQ/mG}(\lambda_1)/S_{df}^{EQ/mG}(\lambda_0)$ represents the sensitivity of Rh^{EQ}/mG rods at λ_1 nm relative to that at λ_0 nm. $\varepsilon_{\lambda_0}^{EQ}\gamma^{EQ}/\varepsilon_{\lambda_0}^{mG}\gamma^{mG}$ is the ratio of photosensitivity at λ_0 nm of E122Q rhodopsin to that of mouse green. C^{EQ}/C^{mG} is the ratio of concentration of E122Q rhodopsin to that of mouse green in the Rh^{EQ}/mG rods (see above, Fig. 6 A).

TABLE III

Response Parameters of Rh^{EQ}/mG Rods for Flashes at Each Wavelength ($n = 14$)

	500 nm pre	600 nm	652 nm	676 nm	500 nm post
Rh^{EQ}: mG (%)	90: 10	31: 69	16: 84	12: 88	90: 10
Dark current (pA)	13.0 ± 0.7	13.3 ± 0.6	13.4 ± 0.5	13.6 ± 0.6	13.6 ± 0.6
Time to peak (ms)	145 ± 4	150 ± 6	146 ± 6	145 ± 5	151 ± 9
Integration time (ms)	276 ± 18	233 ± 18[a]	228 ± 17[a]	228 ± 14[a]	289 ± 18
σ^2/m (pA)	0.48 ± 0.02	0.40 ± 0.03[a]	0.36 ± 0.03[a]	0.30 ± 0.03[b]	0.47 ± 0.03

Rh^{EQ}: mG represents the predicted percentages of E122Q rhodopsin and mouse green photoactivated at each wavelength in Rh^{EQ}/mG rods (see Results). Response parameters were obtained from 14 Rh^{EQ}/mG rods, for each of which stimuli of 500, 600, 652, 676, and 500-nm flashes were delivered in the order. The 500-nm flashes used in the first and the end of the experiment are referred as 500 nm pre and 500 nm post, respectively. The kinetics parameters of single-photon response were taken from dim flash responses, the average of which is $<0.2r_{max}$. σ^2/m is the ensemble variance-to-mean ratio of dim flash stimuli (>30 times) for each wavelength. Values are means ± SEM.
[a]Difference from 500-nm pre flashes being statistically significant, P < 0.05.
[b]Difference from 500-nm pre flashes being statistically significant, P < 0.005. The statistical significance was determined by using the two-tailed paired Student's t test.

Here, we set $\lambda_1 = 600$, 652, or 676 nm and $\lambda_0 = 500$ nm. Then $\varepsilon_{\lambda_1}^{EQ}\big/\varepsilon_{\lambda_0}^{EQ}$ represents the extinction coefficient of E122Q rhodopsin at 600, 652, or 676 nm relative to that at 500 nm, corresponding to the spectral sensitivities at 600, 652, or 676 nm relative to that at 500 nm obtained from Rh^{EQ}/Rh^{EQ} rods. $\varepsilon_{\lambda_1}^{mG}\big/\varepsilon_{\lambda_0}^{mG}$ represents the extinction coefficient of mouse green at 600, 652, or 676 nm relative to the value at 500 nm, corresponding to the spectral sensitivites at 600, 652, or 676 nm relative to that at 500 nm obtained from mG/mG rods. (see above, Table II). $\varepsilon_{\lambda_0}^{EQ}\gamma^{EQ}\big/\varepsilon_{\lambda_0}^{mG}\gamma^{mG}$ represents the ratio of photosensitivity at 500 nm of E122Q rhodopsin to that of mouse green (see above, Fig. 6 B, inset). $S_{df}^{EQ/mG}(\lambda_1)\big/S_{df}^{EQ/mG}(\lambda_0)$ represents the sensitivity of Rh^{EQ}/mG rods at 600-, 652-, or 676-nm light relative to that at 500-nm light.

The values of $S_{df}^{EQ/mG}(\lambda_1)\big/S_{df}^{EQ/mG}(\lambda_0)$ were obtained by single-cell recordings from 14 Rh^{EQ}/mG rods (Table II). According to Eq. 9, the ratio of the amplitude of the elementary response of mouse green to that of E122Q rhodopsin, g_{mG}/g_{EQ}, was calculated to be 0.39 ± 0.05 (mean $\pm$ SEM; $n = 14$). Since the mean amplitude of the single photon response of Rh^{EQ}/Rh^{EQ} rods was 0.80-fold of that of wild-type rods (0.56 pA vs. 0.45 pA; Imai et al., 2007), the ratio of the amplitude of the single photon response of mouse green to that of rhodopsin was estimated to be 0.31, which was comparable to the estimate from the results of wild-type and mG/mG mice.

Thermal Activation of Mouse Green in Green Cone Pigment Knock-in Mice

To evaluate the thermal stability of mouse green, we investigated fluctuation in the membrane current of mG/mG rods and compared it with that of wild-type rods. The measured currents included instrumental and cellular noise. The instrumental noise could be isolated by exposing the rods to a bright saturating light that closed all the channels and completely suppressed the membrane current of the outer segment (Baylor et al., 1980). Thus, we recorded membrane currents from wild-type and mG/mG rods in darkness (Fig. 7, A and B, two top traces) and under saturating lights (Fig. 7 A, two bottom traces, and Fig. 7 B, two middle traces). In addition, we were able to record membrane currents from mG/mG rods where the circulating current was recovered after complete bleach of mouse green (Fig. 7 B, two bottom traces). The extent of the recovery of the membrane current after bleach of various amount of mouse green in mG/mG rods was shown in Fig. 7 E, which implied $\sim$80% recovery of circulating current even after complete bleach of mouse green.

Figs. 7 (C and D) shows the power spectra of these fluctuations. The cellular noise variance within the frequency ranging from 0.3 to 20 Hz, obtained by subtracting the variance under saturating lights from that in darkness, was 0.0046 ± 0.0026 pA^2 (mean $\pm$ SEM; $n = 8$)

for wild-type rods and 0.014 ± 0.0017 pA^2 (mean $\pm$ SEM; $n = 16$; P $<$ 0.005) for mG/mG rods. The value obtained from wild-type rods was comparable to that reported previously (Burns et al., 2002).

It has been reported that the cellular fluctuations in darkness consist of two components: one is a discrete component resembling the single photon response, and the other is a continuously present low amplitude component that probably originates from thermal activations of proteins downstream of the visual pigments (Baylor et al., 1980; Rieke and Baylor, 1996). It was presumed that the power spectrum of cellular dark noise, composed of the former and the latter components, was expressed with a sum of the two functions, Eqs. 4 and 6. First, we evaluated the spectrum of noise derived from thermal activations of mouse green in mG/mG rods by fitting the four-stage independent filter model to dim flash response (Fig. 7 F, inset), and obtained a value of $\alpha = 9.4 \pm 1.9$ s^{-1} (mean $\pm$ SEM) in Eq. 4 from 16 mG/mG rods. Next, we attempted to fit the difference power spectrum of cellular dark noise (Fig. 7 F, closed circles) by a sum of the two functions in Eqs. 4 and 6, where the value of α was fixed as 9.4 s^{-1} and the other values of $Sv(0)$, $Sc(0)$, and β were set as parameters. The solid curve drawn in Fig. 7 F was the calculated fitting curve, where the values were determined as $Sv(0) = 0.0031$ pA^2 Hz^{-1}, $Sc(0) = 0.0029$ pA^2 Hz^{-1}, and $\beta = 33$ s^{-1}. The fitting results indicated that the power spectrum derived from thermal activations of mouse green in darkness was expressed as a function of Eq. 4, with $Sv(0) = 0.0031$ pA^2 Hz^{-1} and $\alpha = 9.4$ s^{-1}. The results also indicated that in darkness the power spectrum derived from the noise component downstream of visual pigment was expressed with the product of two Lorentzians, as described in Eq. 6, with $Sc(0) = 0.0029$ pA^2 Hz^{-1} and $\beta = 33$ s^{-1}, corresponding to a half-power frequency of 3.4 Hz (Fig. 7 F, broken curve); this is similar to the half-power frequency of the continuous component of noise in primate rod ($\sim$3 Hz) (Baylor et al., 1984). Interestingly, the spectrum presumed as the noise component downstream of visual pigment in darkness (Fig. 7 F, broken curve) was well superimposed on the difference power spectrum, calculated by subtracting the spectrum in the presence of saturating light from that after bleaching of visual pigments (Fig. 7 F, open squares). These results indicate that the current fluctuation obtained after complete bleaching of visual pigments followed by recovery of circulating current is comparable to that calculated as a component downstream of visual pigments in darkness.

Since the amplitude of the single-photon response extrapolated from the value of mean r_{max} (7.0 pA) in this experiment was 0.19 pA and the integration time was 0.19 s, the rate of thermal activations of mouse green in mG/mG rod could be estimated to be 1.2 R* s^{-1} from Eq. 5. Given that 7.0×10^6 molecules of mouse

green are present in the outer segment of mG/mG rod (see above), the rate constant of thermal activations of mouse green is estimated to be 1.7×10^{-7} s^{-1}.

In wild-type rods, it was difficult to decompose the spectrum of the cellular dark noise into two components; one from spontaneous activations of rhodopsin and the other from the other continuous component, because thermal activations of rhodopsin are rare events and the cellular noise variance consists predominantly of the continuous component (Baylor et al., 1984; Burns et al., 2002). However the study using mouse rods lacking guanylate cyclase activating proteins (GCAPs), in which the amplitude of the single photon response is much larger relative to the continuous noise, has demonstrated that the rate of thermal activations of rhodopsin is 0.012 R* s^{-1} (Burns et al., 2002). Given 6.1×10^7 molecules of rhodopsin exist in a wild-type rod, the rate constant of this reaction is 2.0×10^{-10} s^{-1}, which is ~860-fold smaller than that obtained from mouse green.

DISCUSSION

The present study clearly showed that the amplitude of single photon response evoked by mouse green was one third of that by rhodopsin, and the rate constant of thermal activation of mouse green in darkness was 1.7×10^{-7} s^{-1}, ~860-fold larger than that of rhodopsin. In the following sections we will discuss the differences in molecular properties between rhodopsin and mouse green that contribute to the photoresponse pattern of rod photoreceptor cells.

Lower Amplitude of the Single-Photon Response in Mouse Green Knock-in Mice

In the present study, we have replaced rhodopsin, one of the factors that affects the response profile of rod photoreceptor cells, with the mouse green cone visual pigment in rod cells. Thus we have experimentally eliminated contributions of the other cone transduction proteins to the photoresponse properties generated by mouse green by introducing the protein into rod cells.

A comparative study between rods and cones of wild-type mice demonstrated that the photosensitivity of rods, specified as a percentage of the circulating dark current suppressed per photoisomerization, is ~25 times larger than that of cones and the time-to-peak and the recovery time constant of rods are three to four times slower than those of cones (Nikonov et al., 2006). On the other hand, replacement of the visual pigment caused a three-fold decrease of photosensitivity but slight effect on the time-to-peak and the recovery time constant. These results suggest that the difference in visual pigment between rods and cones mainly affect the signal amplification of the photoreceptor cells.

Response amplitude of photoreceptor cells is determined both by the efficiencies of signal amplification and active state inactivation. The amplification constant is one of the criteria for the efficiency of signal amplification. It has been reported that the amplification constant of green-sensitive cones is ~2.6-fold smaller than that of mouse rods (Nikonov et al., 2006). Because the amplification constant is inversely proportional to its outer segment volume (Pugh and Lamb, 1993) and the outer segment volume of mouse cones is 0.38-fold smaller than that of mouse rods (Carter-Dawson and LaVail, 1979; Daniele et al., 2005), the volume-normalized amplification constant of cones is ~6.8-fold (2.6 divided by 0.38) smaller than that of the rods (Nikonov et al., 2006). Therefore, our results imply that about half of this 6.8-fold difference in amplification efficiency between rods and cones is ascribed to the difference in molecular properties between rhodopsin and mouse green.

What kinds of molecular properties of visual pigments are related to the amplification constant and amplitude of the single photon response? Photoactivated visual pigments activate many transducins during their lifetimes and their activities are shut down through phosphorylation by G protein–coupled receptor kinase (GRK) (Yau, 1994; Arshavsky et al., 2002). The activation efficiencies of transducin by the active states of rhodopsin and mouse green were compared in the present study (Fig. 4), and these were estimated to be similar with each other. These results are in good agreement with those found in the previous studies (Fukada et al., 1989; Imai et al., 1997; Starace and Knox, 1997). Phosphorylations of rod and cone visual pigments by GRK1 and GRK7 in carp retinas were examined by Tachibanaki et al. (2001, 2005), showing that both pigments were phosphorylated with similar efficiency by GRK1 and GRK7, although GRK1 and GRK7 exhibited enzymatic activities considerably different from each other. It was also reported that the number of residues substantially phosphorylated by GRK1 was apparently identical between rhodopsin and mouse green, although mouse green has two times more putative phosphorylation sites at the C terminus region than rhodopsin (Zhu et al., 2003). Furthermore, the amplitude and shape of rod photoresponses are independent of rhodopsin phosphorylation efficiency as determined by varying the expression level of GRK1 in rods (Krispel et al., 2006). These results strongly suggest that the interactions between visual pigments and other proteins such as transducin and GRK1 are not responsible for the amplitude of photoresponse differences. Therefore, the difference in amplitude of single photon response between wild-type and mG/mG rods should result from the difference in intrinsic properties between rhodopsin and mouse green.

One of the intrinsic molecular properties of visual pigment that affect the amplitude of photoresponse could be the temperature dependence of the equilibrium between the transducin-activating meta-II and its inactive precursor meta-I (Imai et al., 2007). In rhodopsin, the
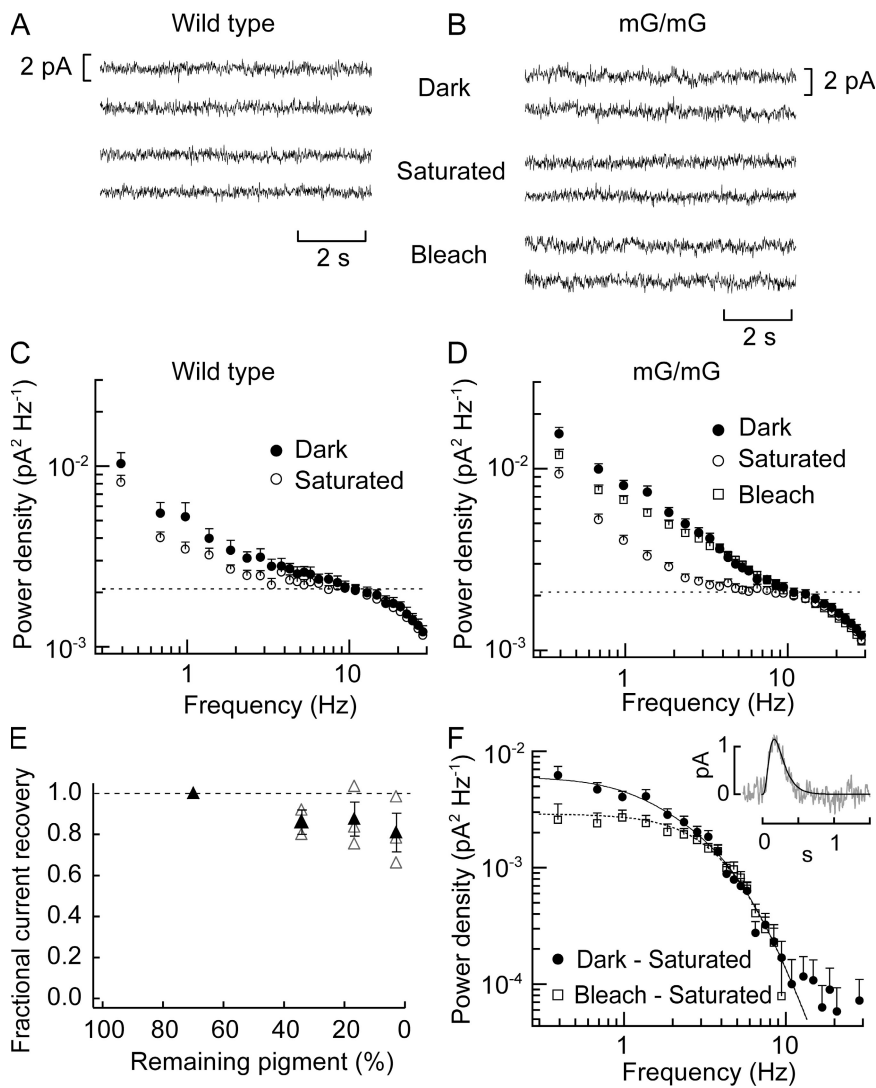
Figure 7. Noise analyses in wild-type and mG/mG rods. (A) Typical traces of membrane currents of wild-type rod in the dark (two top traces) and in the presence of saturating lights (two bottom traces) that close all channels in rod. It should be noted that, in wild-type rods, dark current after bleaching of visual pigments did not recover. The intensity of the saturating 500-nm light was 3.8×10^4 photons $\mu m^{-2} s^{-1}$. The leak resistance was 7.5 MΩ and circulating current was 8.8 pA. (B) Typical traces of membrane currents of mG/mG rod in the dark (two top traces), in the presence of saturating lights (two middle traces), and in darkness after bleaching >99% visual pigments by light irradiation (two bottom traces). The intensity of the saturating 500-nm light was 6.6×10^5 photons $\mu m^{-2} s^{-1}$. The leak resistance was 10.6 MΩ and circulating current was 9.7 pA. (C) Power spectra of current fluctuations calculated from the data of eight wild-type rods in the dark (closed circles) and those in the presence of saturating lights (open circles). The horizontal dotted line denotes the mean Johnson noise level according to the Nyquist equation. The value was 0.0021 $pA^2 Hz^{-1}$ ($n = 8$). (D) Power spectra calculated from the data of 16 mG/mG rods in the dark (closed circles), those in the presence of saturating light (open circle), and those in the dark after bleaching >99% visual pigment (open squares). The horizontal dotted line denotes the mean Johnson noise level according to the Nyquist equation. The value was 0.0021 $pA^2 Hz^{-1}$ ($n = 16$). (E) The recovery of circulating current after bleaching mouse green to various extents in mG/mG rods. The post-bleach circulating currents scaled to the prebleach current were plotted against the amount of remaining pigments. Open triangles indicate the individual data obtained from each cell and closed triangles indicate the data averaged from individual data for given remaining pigments. (F) Difference power spectra derived from mG/mG rods ($n = 16$). The mean difference spectrum calculated by subtracting the power spectrum obtained in the presence of saturating lights from that obtained in darkness is shown as closed circles. The solid curve was drawn according to a sum of Eqs. 4 and 6, with $\alpha = 9.4 s^{-1}$, $\beta = 33 s^{-1}$, $Sv(0) = 0.0031 pA^2 Hz^{-1}$, and $Sc(0) = 0.0029 pA^2 Hz^{-1}$ ($r^2 = 0.97$). The mean difference spectrum calculated by subtracting the power spectrum obtained in the presence of saturating lights from that obtained in darkness after bleaching of visual pigments is shown as open squares. The broken curve was drawn according to Eq. 6 with $\beta = 33 s^{-1}$ and $Sc(0) = 0.0029 pA^2 Hz^{-1}$. (Inset) Application of independent filter function (black traces) to a dim flash response (gray trace) of mG/mG rod. The rate constant of this response was $\alpha = 8.6 s^{-1}$. Error bars indicate SEM. For graphic convenience, only the positive error bars were drawn on the power spectrum data.

equilibrium shifts in favor of meta-II as the temperature of the sample increases. This increases the amount of meta-II to activate transducin. Our previous experiments on bovine rhodopsin showed that the proportion of meta-II in the equilibrium mixture increased approximately two times when the temperature of the sample increases from 0 to 37°C (Morizumi et al., 2005). In contrast, a temperature-dependent shift of the equilibrium was not observed in cone visual pigments (Shichida et al., 1993). Therefore it appears that rhodopsin can activate transducin more than mouse green can at 37°C, whereas it activates transducin with similar extent at 4°C.

Another intrinsic molecular property that may underlie the difference in single photon response amplitude could be the difference in decay time of meta-II between rhodopsin and mouse green. That is, the decay of meta-II of cone visual pigment is considerably faster than that of rhodopsin (Shichida et al., 1994; Imai et al., 1995). Because of the small amount of mouse green in rod outer segments of mG/mG mice, we were unable to monitor the precise decay rate of meta-II of mouse green. However, preliminary experiments indicated that it could be estimated to be <100 ms, which might result in the smaller number of transducins activated by the

meta-II of mouse green than those of rhodopsin before phosphorylation of visual pigments by GRK1.

From a study where human or salamander red-sensitive cone pigments were expressed in *Xenopus* rods, Kefalov et al. (2003) reported that the amplitude of the single photon response generated by the red cone pigment was similar (less than twofold difference) to that by rhodopsin. The discrepancies between their and our results could be due to the difference in animals, rods, and visual pigments with different chromophores between them, although many factors could intricately contribute to the discrepancy. One possibility is the different temperatures used in the measurements. For mammals, the temperature used was 34–38°C and in amphibian it was 20–22°C. As already described, rhodopsin has a tendency to form meta-II at higher temperature but cone visual pigments do not (Shichida et al., 1993). If the similar tendency is applicable to the visual pigments of amphibians whose body temperature is lower than that of mammals, the difference in the response amplitude between rhodopsin and cone visual pigments would become smaller than that in mammals.

Increased Dark Current Fluctuation in Mouse Green Knock-in Rods

According to the noise analysis in the present study, the observed current fluctuations of mG/mG rods are expected to contain two components. One is the current fluctuation derived from the thermal activations of visual pigments and the other is that derived probably from the thermal activations of PDE. As compared with wild-type rods, the variance of both fluctuations was significantly increased in mG/mG rods.

We estimated the rate constant of thermal activation of mouse green in darkness to be $1.7 \times 10^{-7}\,\mathrm{s}^{-1}$, which was ∼860 times larger than that of rhodopsin. On the other hand, this value is ∼300 times smaller than that of salamander red-sensitive cone pigment in native cone cells (Rieke and Baylor, 2000; Sampath and Baylor, 2002) or ∼30 times smaller than A2-based human red in the transgenic *Xenopus* rods (at 37°C) (Kefalov et al., 2003), respectively. These differences could be due to the difference in chromophore and/or absorption maximum (λ_{max}) between mouse green and these red pigments. Visual pigments having A2 chromophore are less stable than those containing A1 chromophore, and the thermal activation rate was expected to be ∼7.6 times higher in A2-based visual pigments than in A1-based visual pigments (Ala-Laurila et al., 2004). In addition, the rate of thermal activation of salamander red-sensitive cone pigment (λ_{max} = ∼620 nm) is expected to be ∼200 times higher than that of the mouse green (λ_{max} = 510 nm), according to the theory that the rate of thermal activation increases exponentially with $1/\lambda_{max}$ (Ala-Laurila et al., 2004).

In contrast to the considerably high thermal activations of mouse green as shown in this study, the cellular fluctuation in blue- or green-sensitive cones arises mainly from the molecular sources downstream from visual pigments rather than the thermal activations of the cone pigments (Lamb and Simon, 1977; Rieke and Baylor, 2000; Holcman and Korenbrot, 2005). There are two possibilities to account for this difference. One is the difference in molecular properties of cone visual pigments among the groups of cone visual pigments. Mouse green as well as salamander red and human red belongs to the L-group (also called M/LWS groups), while the visual pigments in the blue-sensitive and green-sensitive cones mentioned above should belong to the S (short wavelength–sensitive, SWS) and M2 groups (rhodopsin-like [RH2] groups), respectively (Okano et al., 1992; Ebrey and Koutalos, 2001). If a high rate of thermal activations is the unique characteristics of L-group pigments, thermal activation of the visual pigments of other groups do not contribute to current fluctuation in darkness. The other possibility is that the occurrence of the thermal activations of cone pigments even at a considerably high rate is under the limit of detection due to the smaller amplitude of single photon response and larger dark noise from the downstream components in cones.

On the other hand, the increased rate of thermal activations of mouse green in mG/mG rods was accompanied by the increased variance of the downstream component, which would be caused by elevation of the steady PDE activity. Since the increased steady PDE activity is the main factor to accelerate the inactivation of photoresponse and reduce the sensitivity of photoreceptor (Nikonov et al., 2000), it appears that the integration time of dim flash responses in mG/mG rods became slightly faster than that of wild-type rods.

Effect of Spontaneous Dark Activation of Mouse Green on the Adaptation State of Rods

As described above, the low amplitude of photoresponse elicited by mouse green can contribute the threefold difference in sensitivity to the difference between rods and cones. Here we consider one of the other factors that could account for the difference in sensitivity between rods and cones: the effect of thermal isomerizations of the visual pigment chromophore. Thermal isomerization activates the phototransduction cascade, which results in reduction of photosensitivity through a mechanism that is similar to that produced by light (Rieke and Baylor, 2000; Kefalov et al., 2003). Kefalov et al. (2003) reported that rate of spontaneous isomerization of red-sensitive cone visual pigment in salamander rods was ∼175 R* s^{-1}, which could desensitize the rods by six- to sevenfold. On the other hand, desensitization of mouse rods derived from the thermal isomerizations of mouse green would be small as follows.

Our results showed that the rate of thermal activation of mouse green is 1.7×10^{-7} s^{-1}. If all the rhodopsins (6.1×10^7 molecules) present in rod are replaced with mouse green, the rate of spontaneous activation in rod is 10 R* s^{-1}. Because the single photon response generated by mouse green is threefold lower in magnitude than that by rhodopsin, the current change derived from isomerizations of 10 mouse greens is equivalent to that from isomerizations of 3.4 rhodopsins. Therefore, the current noise derived from 10 R* s^{-1} of mouse green should correspond to that from 3.4 R* s^{-1} of rhodopsin. The value 3.4 R* s^{-1} is equivalent to a wild-type rod exposed to a 7.3 photons μm^{-2} s^{-1} of 500-nm background light. In this calculation the effective collecting area (Ac) of rod was estimated to be 0.47 μm^2. The intensity of background light that halves flash sensitivity of mouse rods is $I_B = 178$ photons μm^{-2} s^{-1} (Makino et al., 2004). Therefore, thermal activation of mouse green would slightly shift the intensity/response curve to higher light intensity, resulting in ~4% reduction of the photosensitivity as compared with that of the wild-type rod. This value was estimated from the Weber-Fechner relation; $S_f/S_{fd} = 1/(1 + I/I_B)$, where S_f and S_{fd} are the sensitivities under background illumination and in darkness, respectively. These calculations indicate that the effect of thermal activation of mouse green is not very significant for the adaptation state of rods.

Evolution of Visual Pigments for Scotopic Vision

The phylogenetic tree of vertebrate visual pigments constructed on the basis of amino acid similarity suggests that rhodopsins have diverged from one of the groups of cone visual pigments in the course of molecular evolution (Okano et al., 1992). Thus it is reasonable to speculate that rhodopsin would have acquired unique properties important for scotopic vision. Under dim light conditions where multiple photon absorptions in single rod cells scarcely occur, the high rate of thermal activation and small single-photon responses of mouse green severely affects the ability to detect light signal. Spontaneous thermal activations will generate false-positive signals in visual perception even in the absence of light (Barlow, 1956; Aho et al., 1988). While the absolute threshold of wild-type mouse is 0.001 R* per integration time (Integration time = 200 ms) (Sampath et al., 2005), false positive signals derived from thermal activations in mouse green–containing rods are estimated to be as high as 2.1 R* per integration time. In addition, because the amplitude of single photon response generated by mouse green is about one third of that by rhodopsin and is comparable to the standard deviation of continuous noise (Field and Rieke, 2002), the detection of single photon responses of mouse green would be an extremely challenging event. Taken together, not only the extremely stable nature but also large amplification ability of rhodopsin would be essential when rods have evolved with their ability of the single-photon detection. Therefore we conclude that

rhodopsins acquired two unique properties for mediating scotopic vision during its molecular evolution; one is the extreme stability in darkness and the other is the higher amplification ability for phototransduction.

REFERENCES

Aho, A.C., K. Donner, C. Hyden, L.O. Larsen, and T. Reuter. 1988. Low retinal noise in animals with low body temperature allows high visual sensitivity. *Nature.* 334:348–350.

Ala-Laurila, P., K. Donner, and A. Koskelainen. 2004. Thermal activation and photoactivation of visual pigments. *Biophys. J.* 86:3653–3662.

Applebury, M.L., M.P. Antoch, L.C. Baxter, L.L. Chun, J.D. Falk, F. Farhangfar, K. Kage, M.G. Krzystolik, L.A. Lyass, and J.T. Robbins. 2000. The murine cone photoreceptor: a single cone type expresses both S and M opsins with retinal spatial patterning. *Neuron.* 27:513–523.

Arshavsky, V.Y., T.D. Lamb, and E.N. Pugh Jr. 2002. G proteins and phototransduction. *Annu. Rev. Physiol.* 64:153–187.

Barlow, H.B. 1956. Retinal noise and absolute threshold. *J. Opt. Soc. Am.* 46:634–639.

Baylor, D.A., T.D. Lamb, and K.W. Yau. 1979. Responses of retinal rods to single photons. *J. Physiol.* 288:613–634.

Baylor, D.A., G. Matthews, and K.W. Yau. 1980. Two components of electrical dark noise in toad retinal rod outer segments. *J. Physiol.* 309:591–621.

Baylor, D.A., B.J. Nunn, and J.L. Schnapf. 1984. The photocurrent, noise and spectral sensitivity of rods of the monkey *Macaca fascicularis. J. Physiol.* 357:575–607.

Burns, M.E., A. Mendez, J. Chen, and D.A. Baylor. 2002. Dynamics of cyclic GMP synthesis in retinal rods. *Neuron.* 36:81–91.

Calvert, P.D., V.I. Govardovskii, N. Krasnoperova, R.E. Anderson, J. Lem, and C.L. Makino. 2001. Membrane protein diffusion sets the speed of rod phototransduction. *Nature.* 411:90–94.

Carter-Dawson, L.D., and M.M. LaVail. 1979. Rods and cones in the mouse retina. I. Structural analysis using light and electron microscopy. *J. Comp. Neurol.* 188:245–262.

Choi, T., M. Huang, C. Gorman, and R. Jaenisch. 1991. A generic intron increases gene expression in transgenic mice. *Mol. Cell. Biol.* 11:3070–3074.

Daniele, L.L., C. Lillo, A.L. Lyubarsky, S.S. Nikonov, N. Philp, A.J. Mears, A. Swaroop, D.S. Williams, and E.N. Pugh Jr. 2005. Cone-like morphological, molecular, and electrophysiological features of the photoreceptors of the Nrl knockout mouse. *Invest. Ophthalmol. Vis. Sci.* 46:2156–2167.

Dartnall, H.J. 1968. The photosensitivities of visual pigments in the presence of hydroxylamine. *Vision Res.* 8:339–358.

Donner, K., M.L. Firsov, and V.I. Govardovskii. 1990. The frequency of isomerization-like 'dark' events in rhodopsin and porphyropsin rods of the bull-frog retina. *J. Physiol.* 428:673–692.

Ebrey, T., and Y. Koutalos. 2001. Vertebrate photoreceptors. *Prog. Retin. Eye Res.* 20:49–94.

Field, G.D., and F. Rieke. 2002. Nonlinear signal transfer from mouse rods to bipolar cells and implications for visual sensitivity. *Neuron.* 34:773–785.

Fukada, Y., T. Okano, I.D. Artamonov, and T. Yoshizawa. 1989. Chicken red-sensitive cone visual pigment retains a binding domain for transducin. *FEBS Lett.* 246:69–72.

Govardovskii, V.I., N. Fyhrquist, T. Reuter, D.G. Kuzmin, and K. Donner. 2000. In search of the visual pigment template. *Vis. Neurosci.* 17:509–528.

Hecht, S., S. Shlaer, and M. Pirenne. 1942. Energy, quanta, and vision. *J. Gen. Physiol.* 25:819–840.

Holcman, D., and J.I. Korenbrot. 2005. The limit of photoreceptor sensitivity: molecular mechanisms of dark noise in retinal cones. *J. Gen. Physiol.* 125:641–660.

Hurley, J.B., T.G. Ebrey, B. Honig, and M. Ottolenghi. 1977. Temperature and wavelength effects on the photochemistry of rhodopsin, isorhodopsin, bacteriorhodopsin and their photoproducts. *Nature.* 270:540–542.

Imai, H., Y. Imamoto, T. Yoshizawa, and Y. Shichida. 1995. Difference in molecular properties between chicken green and rhodopsin as related to the functional difference between cone and rod photoreceptor cells. *Biochemistry.* 34:10525–10531.

Imai, H., A. Terakita, S. Tachibanaki, Y. Imamoto, T. Yoshizawa, and Y. Shichida. 1997. Photochemical and biochemical properties of chicken blue-sensitive cone visual pigment. *Biochemistry.* 36:12773–12779.

Imai, H., V. Kefalov, K. Sakurai, O. Chisaka, Y. Ueda, A. Onishi, T. Morizumi, Y. Fu, K. Ichikawa, K. Nakatani, et al. 2007. Molecular properties of rhodopsin and rod function. *J. Biol. Chem.* 282:6677–6684.

Johnson, R.L., K.B. Grant, T.C. Zankel, M.F. Boehm, S.L. Merbs, J. Nathans, and K. Nakanishi. 1993. Cloning and expression of goldfish opsin sequences. *Biochemistry.* 32:208–214.

Kefalov, V., Y. Fu, N. Marsh-Armstrong, and K.W. Yau. 2003. Role of visual pigment properties in rod and cone phototransduction. *Nature.* 425:526–531.

Kodama, T., H. Imai, T. Doi, O. Chisaka, Y. Shichida, and Y. Fujiyoshi. 2005. Expression and localization of an exogenous G protein-coupled receptor fused with the rhodopsin C-terminal sequence in the retinal rod cells of knockin mice. *Exp. Eye Res.* 80:859–869.

Korschen, H.G., M. Illing, R. Seifert, F. Sesti, A. Williams, S. Gotzes, C. Colville, F. Muller, A. Dose, M. Godde, et al. 1995. A 240 kDa protein represents the complete β subunit of the cyclic nucleotide-gated channel from rod photoreceptor. *Neuron.* 15:627–636.

Krispel, C.M., D. Chen, N. Melling, Y.J. Chen, K.A. Martemyanov, N. Quillinan, V.Y. Arshavsky, T.G. Wensel, C.K. Chen, and M.E. Burns. 2006. RGS expression rate-limits recovery of rod photoresponses. *Neuron.* 51:409–416.

Lamb, T.D., and E.J. Simon. 1977. Analysis of electrical noise in turtle cones. *J. Physiol.* 272:435–468.

Lyubarsky, A.L., and E.N. Pugh Jr. 1996. Recovery phase of the murine rod photoresponse reconstructed from electroretinographic recordings. *J. Neurosci.* 16:563–571.

Makino, C.L., R.L. Dodd, J. Chen, M.E. Burns, A. Roca, M.I. Simon, and D.A. Baylor. 2004. Recoverin regulates light-dependent phosphodiesterase activity in retinal rods. *J. Gen. Physiol.* 123:729–741.

Morizumi, T., H. Imai, and Y. Shichida. 2005. Direct observation of the complex formation of GDP-bound transducin with the rhodopsin intermediate having a visible absorption maximum in rod outer segment membranes. *Biochemistry.* 44:9936–9943.

Nikonov, S., T.D. Lamb, and E.N. Pugh Jr. 2000. The role of steady phosphodiesterase activity in the kinetics and sensitivity of the light-adapted salamander rod photoresponse. *J. Gen. Physiol.* 116:795–824.

Nikonov, S.S., L.L. Daniele, X. Zhu, C.M. Craft, A. Swaroop, and E.N. Pugh Jr. 2005. Photoreceptors of Nrl −/− mice coexpress functional S- and M-cone opsins having distinct inactivation mechanisms. *J. Gen. Physiol.* 125:287–304.

Nikonov, S.S., R. Kholodenko, J. Lem, and E.N. Pugh Jr. 2006. Physiological features of the S- and M-cone photoreceptors of wild-type mice from single-cell recordings. *J. Gen. Physiol.* 127:359–374.

Okano, T., Y. Fukada, I.D. Artamonov, and T. Yoshizawa. 1989. Purification of cone visual pigments from chicken retina. *Biochemistry.* 28:8848–8856.

Okano, T., D. Kojima, Y. Fukada, Y. Shichida, and T. Yoshizawa. 1992. Primary structures of chicken cone visual pigments: vertebrate rhodopsins have evolved out of cone visual pigments. *Proc. Natl. Acad. Sci. USA.* 89:5932–5936.

Onishi, A., J. Hasegawa, H. Imai, O. Chisaka, Y. Ueda, Y. Honda, M. Tachibana, and Y. Shichida. 2005. Generation of knock-in mice carrying third cones with spectral sensitivity different from S and L cones. *Zoolog. Sci.* 22:1145–1156.

Pugh, E.N., Jr., and T.D. Lamb. 1993. Amplification and kinetics of the activation steps in phototransduction. *Biochim. Biophys. Acta.* 1141:111–149.

Rieke, F., and D.A. Baylor. 1996. Molecular origin of continuous dark noise in rod photoreceptors. *Biophys. J.* 71:2553–2572.

Rieke, F., and D.A. Baylor. 2000. Origin and functional impact of dark noise in retinal cones. *Neuron.* 26:181–186.

Sampath, A.P., and D.A. Baylor. 2002. Molecular mechanism of spontaneous pigment activation in retinal cones. *Biophys. J.* 83:184–193.

Sampath, A.P., K.J. Strissel, R. Elias, V.Y. Arshavsky, J.F. McGinnis, J. Chen, S. Kawamura, F. Rieke, and J.B. Hurley. 2005. Recoverin improves rod-mediated vision by enhancing signal transmission in the mouse retina. *Neuron.* 46:413–420.

Shichida, Y., H. Imai, Y. Imamoto, Y. Fukada, and T. Yoshizawa. 1994. Is chicken green-sensitive cone visual pigment a rhodopsin-like pigment? A comparative study of the molecular properties between chicken green and rhodopsin. *Biochemistry.* 33:9040–9044.

Shichida, Y., T. Okada, H. Kandori, Y. Fukada, and T. Yoshizawa. 1993. Nanosecond laser photolysis of iodopsin, a chicken red-sensitive cone visual pigment. *Biochemistry.* 32:10832–10838.

Shichida, Y., T. Ono, T. Yoshizawa, H. Matsumoto, A.E. Asato, J.P. Zingoni, and R.S. Liu. 1987. Electrostatic interaction between retinylidene chromophore and opsin in rhodopsin studied by fluorinated rhodopsin analogues. *Biochemistry.* 26:4422–4428.

Starace, D.M., and B.E. Knox. 1997. Activation of transducin by a *Xenopus* short wavelength visual pigment. *J. Biol. Chem.* 272:1095–1100.

Suzuki, T., K. Narita, K. Yoshihara, K. Nagai, and Y. Kito. 1993. Immunochemical detection of GTP-binding protein in cephalopod photoreceptors by anti-peptide antibodies. *Zoolog. Sci.* 10:425–430.

Tachibanaki, S., D. Arinobu, Y. Shimauchi-Matsukawa, S. Tsushima, and S. Kawamura. 2005. Highly effective phosphorylation by G protein-coupled receptor kinase 7 of light-activated visual pigment in cones. *Proc. Natl. Acad. Sci. USA.* 102:9329–9334.

Tachibanaki, S., H. Imai, T. Mizukami, T. Okada, Y. Imamoto, T. Matsuda, Y. Fukada, A. Terakita, and Y. Shichida. 1997. Presence of two rhodopsin intermediates responsible for transducin activation. *Biochemistry*. 36:14173–14180.

Tachibanaki, S., S. Tsushima, and S. Kawamura. 2001. Low amplification and fast visual pigment phosphorylation as mechanisms characterizing cone photoresponses. *Proc. Natl. Acad. Sci. USA*. 98:14044–14049.

Terakita, A., T. Yamashita, S. Tachibanaki, and Y. Shichida. 1998. Selective activation of G-protein subtypes by vertebrate and invertebrate rhodopsins. *FEBS Lett.* 439:110–114.

Usukura, J., and E. Yamada. 1987. Ultrastructure of the synaptic ribbons in photoreceptor cells of *Rana catesbeiana* revealed by freeze-etching and freeze-substitution. *Cell Tissue Res.* 247:483–488.

Yau, K.W. 1994. Phototransduction mechanism in retinal rods and cones. The Friedenwald Lecture. *Invest. Ophthalmol. Vis. Sci.* 35:9–32.

Zhu, X., B. Brown, A. Li, A.J. Mears, A. Swaroop, and C.M. Craft. 2003. GRK1-dependent phosphorylation of S and M opsins and their binding to cone arrestin during cone phototransduction in the mouse retina. *J. Neurosci.* 23:6152–6160.